Assessment of plant water status variability by thermography:

Comparing ground measurements with remote imaging

Irene Rodschinka

Dissertation to obtain the degree of

European Master of Science in Viticulture and Enology

Supervisor: Professor Carlos Lopes / Instituto Superior de Agronomia Lisboa

Supervisor in the hosting organisation: Professor Stefano Poni / Università Cattolica del Sacro Cuore

Jury:

President:	Jorge Manuel Rodrigues Ricardo da Silva (PhD), Full Professor, Instituto Superior de Agronomia, Universidade de Lisboa
Members:	Manfred Stoll (PhD), Full Professor, Hochschule Geisenheim University
	Carlos Manuel Antunes Lopes (PhD), Associated Professor with habilitation, Instituto Superior de Agronomia, Universidade de Lisboa
	Joaquim Miguel Rangel da Cunha Costa (PhD), Assistant Professor, Instituto Superior de Agronomia, Universidade de Lisboa

2018

Acknowledgements

I would like to acknowledge my indebtedness and render my warmest thanks to my supervisor in the hosting organisation, Professor Stefano Poni, who suggested and realized this work. His guidance and expert advice have been invaluable throughout the stages of the work.

I would also wish to express my gratitude to Professor Matteo Gatti for extended discussions and valuable suggestions which have contributed greatly to the improvement of the thesis.

The thesis has also extensively benefited from the technical support and expertise from Alessandro Matese of Italian National Research Council (CNR), Firenze, and his team. The same applies to the staff at the 'Centro di Ricerca Analisi geoSpaziale e Telerilevamento' (CRAST) in Piacenza.

This thesis has been written during my stay at Università Cattolica di Piacenza. I would like to thank the Viticulture Department for providing excellent working conditions, and Istituto Toniolo with 'Borsa Invernizzi' for its financial support.

Abstract

Remote sensing provides a fast alternative for traditional in situ water status measurement in vineyards. Canopy temperature measurements derived from aerial thermography were compared to thermal and plant physiological ground-truthing data of single vines in a low and high vigour zone. The experimental trial was carried out in a vineyard of Colli Piacentini, located in the province of Piacenza (Italy). Statistical methods were used to evaluate the correlation between acquired temperatures and plant physiological parameters. Results by simple regression showed significant correlation, with coefficient of determination (R^2) higher than 0.6 for the indices studied; R^2 higher than 0.7 for correlations of thermal data with vine water status' and R^2 higher than 0.9 for correlations deriving from data of vines of the high vigour zone. These results propose that thermography is a good estimator for vine water status and photosynthetic activity. However, records of aerial and proximal thermal imaging are not congruent but have a similar behaviour and correlation when comparing to ground measurements. Therefore, when only using thermography, vine water stress is not only indicated by a higher canopy temperature in absolute values but is an implication of temperature variation within the field over time. Comparative measurements can improve assessing vine water status by observing changes in canopy temperature.

Key words: remote sensing, thermography, vine water status

Síntese

O sensoriamento remoto pode fornecer uma alternativa rápida para a medição tradicional do estado da água em vinhedos. As medidas de temperatura do dossel derivadas da termografia aérea foram comparadas com os dados fisiológicos térmicos e fitossanitários da videira em uma zona de baixo e alto vigor. O experimento foi realizado em um vinhedo de Colli Piacentini, localizado na província de Piacenza (Itália). Métodos estatísticos foram utilizados para avaliar a correlação entre temperaturas adquiridas e parâmetros fisiológicos das plantas. Os resultados por regressão simples mostraram correlação significativa, com coeficiente de determinação (R^2) maior que 0,6 para os índices estudados; R^2 superior a 0,7 para correlações de dados térmicos com o estado da água da vinha e R^2 superior a 0,9 para correlações decorrentes de dados de videiras da zona de alto vigor. Estes resultados sugerem que a termografia é um bom estimador para o estado da água e para a atividade fotossintética. No entanto, os registros de imagens térmicas aéreas e proximais não são congruentes, mas tem um comportamento e correlação semelhantes quando comparados às medições do solo. Portanto, quando se usa apenas termografia, o estresse hídrico da vinha não é indicado apenas por uma temperatura de dossel mais alta em valores absolutos, mas é uma implicação da variação de temperatura dentro do campo ao longo do tempo. Medições comparativas podem melhorar a avaliação do estado da água da vinha observando as mudanças na temperatura do dossel.

Palavras-chave: sensoriamento remoto, termografia, estado da água da vinha

Resumo alargado

O estado da água da vinha tem implicações nos parâmetros de rendimento e de qualidade e é, portanto, essencial para a economia da gestão da vinha. O stress do défice hídrico na videira pode evocar um crescimento limitado do rebento, peso das bagas, composição da uva e qualidade geral da vindima. Assim, uma ferramenta precisa e fácil de implementar para avaliar o estado hídrico da videira pode clarificar o nível de stress das plantas e pode levar a uma adaptação da gestão adequada do copado, à redução da produção ou à implementação da irrigação deficitária. A tese seguinte trata de métodos para a detecção do stress hídrico e do estado da água e testa a sua aplicabilidade e fiabilidade. Entre os métodos existentes, o estado hídrico da vinha foi avaliado ao meio-dia e pré-dia e foram efectuadas medições do potencial hídrico das folhas e da temperatura das folhas, uma vez que a temperatura das folhas é importante como indicador de aspectos da função fisiológica, especialmente os relacionados com a taxa de evaporação e abertura estomática, com as temperaturas a diminuir à medida que os estomas se abrem e as taxas de evaporação aumentam. Aqui, dois métodos diferentes de aplicação da chamada termografia foram utilizados: Medições térmicas a partir da vizinhança imediata com uma câmera portátil e medições térmicas de maior distância por drone.

A questão foi formulada, como o stress hídrico exibido pelo estado da água da planta e sua variabilidade é reproduzido em uma variabilidade da temperatura da copa e se esta avaliação não invasiva e remota por termografia é capaz de concluir de forma confiável o estado da água da videira.

Neste estudo, as medições da temperatura do dossel derivadas da termografia aérea foram comparadas com os dados fisiológicos térmicos e fitossanitários das videiras individuais numa zona de baixo e alto vigor. O ensaio experimental foi realizado numa vinha de Colli Piacentini, localizada na província de Piacenza (Itália). Foram utilizados métodos estatísticos para avaliar a correlação entre as temperaturas adquiridas e os parâmetros fisiológicos das plantas. Os resultados por regressão simples mostraram correlação significativa, com coeficiente de determinação (R2) superior a 0,6 para os índices estudados; R2 superior a 0,7 para correlações dos dados térmicos com o estado hídrico da vinha' e R2 superior a 0,9 para correlações derivadas dos dados das videiras da zona de alto vigor. Estes resultados propõem que a termografia é um bom e rápido estimador do estado da água da vinha e da actividade fotossintética e uma valioso instrumento não invasivo na viticultura de precisão. As principais vantagens destes métodos são a facilidade de implementação, processamento e resposta imediata.

Portanto, o estabelecimento de relações entre parâmetros fisiológicos como a taxa fotossintética e o estado hídrico das videiras apresentadas fornecem uma base sólida para a determinação do estado hídrico.

Todavia, entre os métodos de termografia, os registos de imagens térmicas aéreas e proximais não são congruentes, mas têm um comportamento e correlação congruentes quando comparados com as medições do solo.

No entanto, qualquer estudo dos processos fisiológicos deve ter em conta a sensibilidade da temperatura do processo em relação à variação natural (espacial e temporal) da temperatura. O uso de um valor absoluto da temperatura da folha como indicador da condutância ou transpiração do estômago, no entanto, é pouco significativo pelo facto de a temperatura da folha ser também afectada por uma vasta gama de outras características vegetais e ambientais de acordo com o balanço energético da folha e especialmente pela variação do valor da temperatura devido à diferente imaginação óptica do dossel. Além disso, como o ambiente está em constante variação, pelo menos para as plantas no campo, torna-se também necessário considerar o comportamento dinâmico da temperatura da folha em qualquer estudo preciso da temperatura da folha. Assim, quando se utiliza apenas a termografia, o stress hídrico da vinha não é apenas indicado por uma temperatura de copa mais elevada em valores absolutos, mas é uma implicação da variação da temperatura no campo ao longo do tempo. As medições comparativas podem melhorar a avaliação do estado da água da vinha através da observação de alterações na temperatura do dossel.

Table of Contents

List of Figures

List of Tables

List of Equations

Aim of the Research Project

Vine water status has implications on yield and quality parameters and is therefore essential to the economics of vineyard management. Water deficit stress on grapevine can evoke limited shoot growth, berry weight, grape composition and overall vintage quality. Therefore, an accurate and easy-to implement tool for assessing vine water status can clarify the stress level of the plants and could lead into an adaption of appropriate canopy management, yield reduction or the implementation of deficit irrigation.

The following thesis deals with methods for the detection of water stress and water status and tests their applicability and reliability. Among existing methods, vine water status was assessed by midday and pre-dawn leaf water potential and leaf temperature measurements were undertaken, as leaf temperature is important as an indicator of aspects of physiological function, especially those related to evaporation rate and stomatal opening, with temperatures decreasing as stomata open and as evaporation rates increase. Here, two different methods of so called thermography application were used: Thermal measurements from the immediate vicinity with a handheld camera and thermal measurements of greater distance by drone.

The question has been formulated, how water stress displayed by plant water status and its variability is reproduced in a variability of canopy temperature and if this non-invasive and remote assessment by thermography is able to conclude reliably vine water status.

1. Literature Review

This chapter reviews the underlying physiological and technological knowledge currently supporting ground-truthing practice in vineyards which, on the other hand, are used to examine reliability of thermal data acquired by remote sensing thermography.

As an introduction plant hydraulics and the water movement through the grapevine from the soil to the atmosphere by plant vascular structures are reviewed. Known mechanisms of adaptation to water stress are reported and placed in the context of proximal and remote sensing strategies.

1.1 Hydraulic Architecture of Grapevines

Studying the water use of plants, the Soil-Plant-Atmosphere-Continuum (SPAC) is a key concept: The conception of the SPAC arises from the cohesion-tension theory (CT) of water movement through plants (Dixon & Joly, 1894) and the comprehension of water moving from soil into roots, through plants and into the atmosphere along gradients in water potential. A summary of the pathway of water transport from the soil, through the plant and to the atmosphere is presented in figure 1 and is assessed in this section in terms of plant hydraulics.

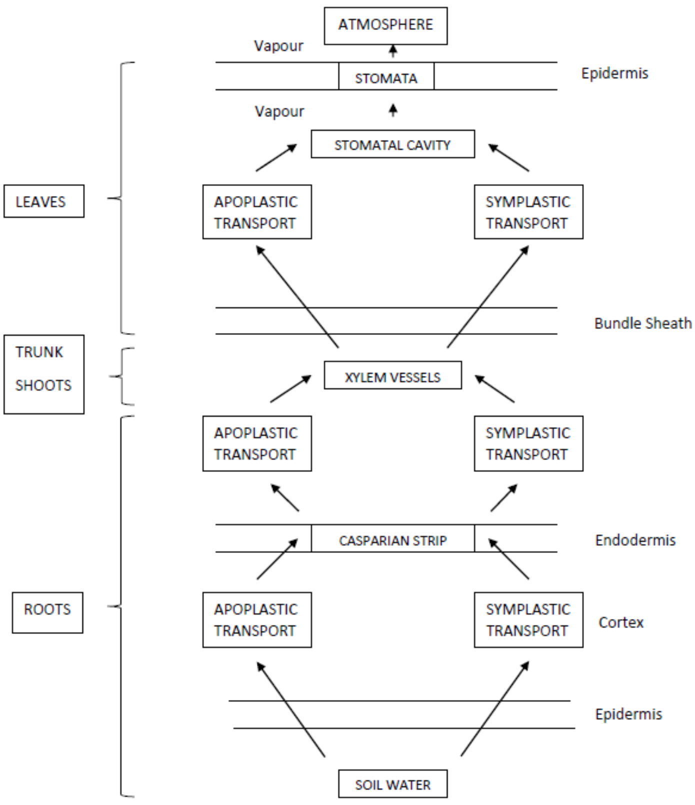

Figure 1 Summary of the Soil Plant Atmosphere Continuum (SPAC)

Water moves from the soil through the cortex using apoplastic (outside the cell membrane) and symplastic (inside the cell membrane) paths, across the casparian strip and enters the xylem (Salisbury & Ross, 1992). Driven by a combination of the transpiration stream and osmotic potential, the water in leaf's xylem moves towards the stomatal cavities where it diffuses into the atmospheric boundary layer located around the leaf (Guisard, 2008).

1.1.1 Energetics of the Hydraulic System

The state of a hydraulic system can be described in terms of the amount of water it contains (often termed its 'water content') and its energetic (or qualitative) component (Campbell & Norman, 1998).

The energy status within a component of the hydraulic system can be represented using the concept of water potential (Ψ) (Slatyer & Taylor, 1962). Pure water at atmospheric pressure has a solute potential of zero. As solute is added, the value for solute potential becomes more negative, but increased pressure will increase it (making it less negative). Unless hindered, water will move from an area of high to low water potential. The water potential within a plant is generally negative as defined using the simplified equation:

$$\Psi = \Psi_0 + \Psi_P$$

(Equation 1)

where Ψ_O is the osmotic potential

Ψ_P is the pressure potential

Within the Soil Plant Atmosphere Continuum (SPAC), many elements of different hydraulic conductance and capacitance such as the contribution of individual roots, shoots or leaves can be identified. Resistances placed in series are additive ($R = R_1 + R_2 + \dots R_n$). Resistances placed in parallel can be calculated as the reciprocal of the sum of the reciprocals of the individual resistances (figure 2) (Campbell & Norman, 1998).

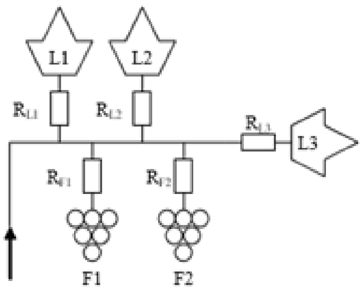

$$R = \frac{1}{\frac{1}{RL1} + \frac{1}{Rl2} + \frac{1}{RL3} + \frac{1}{RF1} + \frac{1}{RF2}}$$

Figure 2 Resistance to water flow in the plant. R represents the equivalent resistance to the parallel petiole resistance to water flow into leaves (L1, L2, L3) and fruits (F1, F2)

1.1.2 Characterising Hydraulic Parameters of Grapevines

1.1.2.1 Hydraulic Conductivity of Plant Stems

Tyree and Ewers (1991) and Jones (1992), proposed to use the Poiseuille's law to model the hydraulic behaviour of a bundle of cylindrical xylem vessels:

$$k_h = \left(\frac{\pi\rho}{128\eta}\right) \sum_{i=1}^{n} d\ ^{4}{}_{1}$$

(Equation 2)

where k_h is the hydraulic conductivity of a bundle of pipes of various diameters ($kg.s^{-1}.MPa^{-1}$)
ρ is the density of the fluid ($kg.m^{-3}$)
ŋ is the dynamic viscosity of the fluid ($MPa.s^{-1}$)
d is the diameter of each pipe (xylem vessel) (m)
n is the number of pipes

This equation demonstrates the factorial impact of a large vessel diameter on hydraulic conductivity.

Plant leaves contain tiny openings called stomata (singular 'stoma' or 'stomate') mostly found on the underside of leaf blades (hypostomatous). Stomata open and close to allow the intake of carbon dioxide from the atmosphere and the release of oxygen and water vapour.

If well hydrated leaves have a high water potential and if evaporative demand increases through the day, the plant will need to contribute with water reserves and hydraulic conductivity for the stomata to remain open and the leaf to stay well hydrated.

The Huber Value (HV) (Huber, 1928, cited in Cruiziat et al., 2002) measures a plant's investment in stem tissue per unit of leaf area (equation adapted from Tyree & Ewers, 1991):

$$HV = \frac{LSC}{Ks}$$

(Equation 3)

where HV is dimensionless
LSC is the Leaf Specific Conductivity ($kg.s^{-1}.MPa^{-1}.m^{-2}$)

LSC and K_s can be defined by:

$$LSC = \frac{Kh}{AL}$$

(Equation 4)

$$K_s = \frac{Kh}{Aw}$$

(Equation 5)

where K_h is the hydraulic conductivity per unit pressure gradient as defined in (Equation 2) and (Equation 3)

A_w is the area of the sap wood cross section (m^2)

A_L is the leaf area fed by the sap wood cross section considered by A_w (m^2)

When the evaporative flux density E ($kg.s^{-1}.m^{-2}$) is known and ignoring the water storage capacitance of a stem segment, it can be shown that:

$$\frac{dP}{dx} = \frac{E}{LSC}$$

(Equation 6)

where dP/dx is the pressure gradient per unit length

Equation 1.6 demonstrates that for a given leaf surface area, plants with a high hydraulic conductivity can evaporate a given flux density of water using less pressure gradient per unit length than plants with low leaf surface area.

Putting together (Equation 4), (Equation 5) and (Equation 6), the Huber Value (HV) can now be solved for stem and leaf areas (A_w and A_L):

$$HV = \frac{Aw}{Al}$$

(Equation 7)

A low Huber Value (HV) would therefore indicate high stem conductivity and the capacity to transport water to a set value for A_L using small stem diameters. Variability of the Huber Value was found to be high across but also within plant species (Cruiziat et al., 2002).

<u>1.1.2.2 Xylem</u>

A general agreement in literature prevails over the major source of xylem hydraulic resistance (regardless of the plant organ) Xylem cavitation or xylem embolism evokes a rupture of the water column and it is due to xylem vessels filling up with air or dissolved gases (Tyree & Ewers, 1991).

1.1.2.3 The Hydraulic Regulation

Reduced hydraulic conductivity is caused by sites of higher hydraulic resistance such as the root system identified by Liu (1978) as the largest cause of resistance on Vitis labrusca. Lovisolo & Schubert (1998) noted that the stem xylem vessels diameters (K_h in Poiseuille's law) contribute very much to a reduction of hydraulic conductivity as it is factorial included in the Poiseuille's law. This approach has been also suggested by the experimental work of Schultz (1983).

Sack & Holbrook (2006) argued that for most plants, leaves are a major contributor to the whole plant hydraulic resistance to water flow for several reasons:

- The resistance of stomata to water vapour flow from the stomatal cavity to the surrounding boundary layer is extremely large when compared to bulk flow, even when the stomata are fully opened.
- Leaves have the ability to control vapour diffusion rate via stomatal behaviour, further increasing resistance when stomata close in response to water stress (Guisard, 2008).

1.1.3 Summary and Conclusions

This chapter reviewed the hydraulic properties of plants with regard to conducting vessels subjected to driving forces and regulated by leaf stomata.

As defining the dominant hydraulic resistance at increasing water stress becomes more complex and variable due to the grapevines hydraulic structure, the assessment of vine water status is unlikely a simple growers' routine unless the drivers and resistances can be accurately modelled.

In the following chapter the knowledge of the mechanisms of stomatal regulation in grapevine and its adaptation to water stress is reviewed in detail.

1.2 Plant Responses to Water Stress

In this section, the general plant adaptive responses to increasing water stress will be presented followed by a detailed examination of the mechanism of stomatal control of water use.

1.2.1 Plant Adaptation to Drought

Droughts, periods of sub-maximal plant water potential, are classified in the literature as being short or long term (Chaves et al., 2003). Short droughts (ranging from hours to a day) tend to induce metabolic protective responses (usually reversible) whilst slowly induced, long term droughts (ranging from several days to months) tend to induce potentially irreversible adaptive responses (Guisard, 2008). Short term droughts provoke growth arrest as a primary response and induce genetic response for metabolic acclimation and induce osmotic adjustments. Jones (1992) reported short term droughts to be associated with potent stomatal control of stomatal behaviour.

Plant-water relations or drought resistance of C3 mesophytes can be generally divided into a drought avoiding or drought tolerating behaviour (Salisbury & Ross, 1992).

Drought avoiding plants, also termed 'pessimistic' or isohydric plants (Escalona et al., 1999), modify their anatomy (leaf shape, size and thickness) and phenology (early flower set, fruit ripening and/or leaf fall), to conserve available water resources (Cifre et al., 2005). Drought tolerant plants, also termed 'optimistic plants', use all available water in expectation of upcoming rain. This is achieved by maintaining cell turgor and favours the use of protective solutes and desiccation tolerant enzymes (Escalona et al., 1999). This behaviour is called anisohydric. In general, grapevine is considered a water stress avoidant species, with a tight stomatal control. However, some varieties have shown a more efficient stomatal control than others. This encouraged researchers to classify grapevine varieties as isohydric or anisohydric. Table 1 is a summary of the various regions of stomatal regulation as a function of drought severity.

Table 1 Summary of the impact of drought severity on stomatal regulation. From Medrano et al., (2002)

Drought severity	Stomatal conductance (mmol m^{-2} s^{-1})	Type of regulation
Mild stress	0,4 - 0,15	Stomatal regulation
High stress	0,15 - 0,05	Stomatal and non-stomatal regulation
Severe stress	< 0,05	Non-stomatal regulation

Mild water stress in grapevines has been shown to induce a reduction in vegetative growth (Deloire, Carbonneau, Wang, & Ojeda, 2004; Galet, 1993; Schultz, 1983) and to affect reproductive growth and to reduce yields (Bravdo, Hepner, Loigner, & Tabacman, 1985; Galet, 1993; Hardie & Considine, 1976; Matthews & Anderson, 1988). Extreme water stress leads to defoliation and vine exitus (Le Clech, 1996).

From a hydraulic resistance perspective, the central role of the stomata was highlighted in the previous section. It is now highlighted in regard to optimising the balance between water loss by transpiration and CO_2 uptake (Chaves et al., 2003; Chaves et al., 2002; Jones, 1998; Loveys, 2002; Guisard, 2008).

In the following Figure 3 the control mechanisms to regulate water and CO_2 fluxes as a result of environmental (feed forward) and physiological (feedback) circuits are summarized.

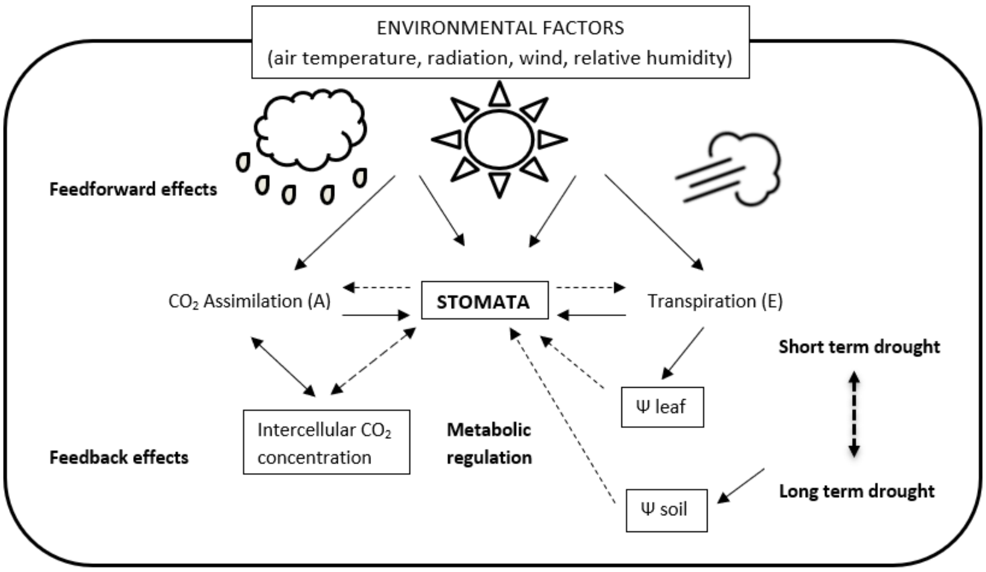

Figure 3 Summary of feed forward and feedback mechanisms of stomatal control of CO_2 assimilation and water vapour losses. Plain lines indicate direct effects, and dotted lines indicate indirect effects. Adapted from Jones (1992, 1998)

The shown mechanisms of stomatal control are the subject of various mechanistic models that will now be presented.

1.2.2 Environmental Influences on Stomatal Resistance

The effect of air temperature on stomatal conductance in the field is usually difficult to isolate from the relative humidity effects. This difficulty can be overcome by using growth chambers, as is the case for helox based studies (Guisard, 2008).

The relationship between stomatal conductance and relative humidity has raised strong debates in the literature. The vapour pressure deficit (VPD, in kPa) is defined as the difference in vapour pressure between saturated and ambient air at air temperature (Campbell & Norman, 1998):

$$VPD = e_s(T_a) - e_a = e_s(T_a)(1-h_r)$$

(Equation 8)

where e_s (Ta) is the saturated vapour pressure (kPa)

e_a is the ambient air vapour pressure (kPa)

T_a is the ambient temperature (°C)

h_r is the relative humidity

Saturated vapour pressure at ambient temperature ($e_s(T_a)$) can be computed as a function of air temperature (Campbell & Norman, 1998):

$$e_s(Ta) = 0.611 exp\left(\frac{17.502Ta}{Ta+240.97}\right)$$

(Equation 9)

Equation 8 and Equation 9 demonstrate the close relationship between air temperature and VPD and the intrinsic difficulty to separate both effects in the field when ambient VPD is measured as a predictive variable.

Literature in grapevine studies reports on the negative relationship between VPD and stomatal conductance (Gomez del Campo et al., 2004; Jacobs, van den Hurk, & de Bruin, 1996; Kliewer et al., 1983; Loveys, 2002; Lu et al., 2003; Guisard, 2008).

1.2.3 Environmental Influences on CO_2 Assimilation

Photosynthesis in grapevines displays a typical rectangular hyperbolic response to exposure to light intensity (Kriedemann, 1968) with a compensation point (where net photosynthesis becomes positive) at about 50 μmol.m^{-2}.s^{-1} (Mullins et al., 1992).

However, adaptation to high light intensity is variable with maximum reported values ranging from 690 μmol.m^{-2}.s^{-1} (cv Sultana) (Kriedemann, 1968) to 1800 μmol.m^{-2}.s^{-1} (cv Tempranillo) (Baeza et al., 2005). Palliotti et al., (2000; 2001) reported an adaptation to constant low light for the shaded sides of canopies, measured as a saturation value around 200 μmol.m^{-2}.s^{-1}.

Mullins (1992) and Kriedemann (1968) reported that air temperature ranging between 25°C to 30°C was optimal for leaf function, but outside this range photosynthesis was reduced. Ferrini et al., (1995) reported similar responses although these authors highlighted the variability of responses between cultivars.

1.2.4 Models of Stomatal Response to Environmental Factors

A model based upon the linear feed forward sensitivity of the stomata of some plants to VPD was proposed by Ball, Woodrow, and Berry (1987):

$$g_s = g_0 + kA_{n,\ leaf}\frac{hs}{Cca}$$

(Equation 10)

where g_0 is the residual stomatal conductance (mol.m^{-2}.s^{-1})
k is a stomatal sensitivity factor
A_n, leaf is the net carbon assimilation by a leaf (mol.m^{-2}.s^{-1})
h_s is the VPD at the leaf surface (mol.mol^{-1})
C_{ca} is the ambient air CO_2 concentration (mol.mol^{-1}) (approximately 350 μmol.mol^{-1})

Considering that stomatal aperture is also regulated as well as limited by the capacity of C3 plants to fix carbon (Campbell & Norman, 1998; Wong et al., 1979) was leading to various similar models:

$$A_{n,\ leaf} = g_c\ (C_{ca} - C_{ci})$$

(Equation 11)

where $A_{n,\ leaf}$ is the net carbon assimilation by a leaf (mol.m^{-2}.s^{-1})
g_c is stomatal and boundary conductance (in series) (mol.m^{-2}.s^{-1}) for CO_2
C_{ci} is the mesophyll CO_2 concentration (mol.mol^{-1})

C_{ci} is reported to saturate around 280 μmol.mol^{-1} in C3 plants (Campbell & Norman, 1998), and was reported by Düring (2003) to saturate in Riesling leaves at 340 μmol.mol^{-1}.

1.2.5 Feedback mechanisms of stomatal control

Various studies have proposed that stomatal conductance is regulated by the plant's hydraulic system. Jones (1992, 1998) proposed a simple linear model suggesting that stomatal conductance is regulated by leaf water potential:

$$g_s = g_m\,(1 + k\Psi_{leaf})$$

(Equation 12)

where g_m is the maximum stomatal conductance (mol.m^{-2}.s^{-1})

Ψ_{leaf} is the leaf water potential (MPa)

k = 0.4 MPa^{-1}

However, leaf water potential control represents only part of the control mechanisms. Jones (1992, 1998) therefore proposed the use of g_s as a predictor variable:

$$\Psi_{leaf} = \Psi_{soil} - VPD\, g_s\, R_{soil\text{ - }plant}$$

(Equation 13)

where Ψ_{soil} is the soil water potential (MPa)

$R_{soil\text{ - }plant}$ is the frictional loss in the conducting pathway (MPa.m^{-2}.s.mol^{-1})

Solving simultaneously Equation 12 and Equation 13 demonstrates that VPD and Ψ_{soil} are the driving variables of the system, linked by Ψ_{leaf}. However, more recently, Jones (2007) presented a new hypothesis that water potential is unlikely to be the cause of stomatal sensitivity, but rather that changes in cell turgor pressure or cell volume that accompany changes in water potential are the direct cause.

1.2.5 Summary and Conclusions

This section has described grapevines' adaptation to increasing levels of water stress in terms of anatomical adaptations as well as biochemical regulation of stomatal function via the feed forward and feedback processes.

It has been shown that feed forward mechanisms act linearly on stomatal conductance and react with environmental factors (wind speed, air temperature, VPD and solar radiation). In the presence of water stress, feedback mechanisms predominant over direct relationships to regulate the balance between CO_2 intake and water loss. Water potential is highly likely to be the mechanistic link between supply (soil water) and environmental demand (VPD), although leaf temperature was also suggested.

To assess the actual condition of the vine growers will continue to rely on measures of the expression of one or several of the processes described above as indicators of the water status of the vine. The next section describes the indicators of water stress currently used or having potential to be used for irrigation scheduling purposes.

1.3 Plant Based Indicators of Water Stress

Various plant-based indicators can be evaluated to understand vineyard's plant water status. As a consequence, winegrowers can come into action regarding irrigation purposes. The plant-based indicators will now be reviewed.

1.3.1 Water Potential

In section 1.1.1 'plant water status' got incorporated into its attributes of its water 'content' and its energy status. To indicate energy status the concept of water potential related to solute flow in the plant hydraulic system (Equation 2) was introduced. In the following water potential measures will be reviewed.

1.3.1.1 Leaf Water Potential

Leaf water potential Ψ_{leaf} is by far the most reported plant-based water stress indicator reported in the literature and is usually measured using a pressure chamber (Scholander, et al., 1965; Waring & Cleary, 1967).

The use of this plant-based indicator is also justified due to the probable involvement of Ψ_{leaf} in feedback process of stomatal regulation. Indeed, the diurnal behaviour of Ψ_{leaf} has been used to classify grapevine cultivars into isohydric and anisohydric groupings (Schultz, 2003).

On the other hand, the Ψ_{leaf} of anisohydric cultivars (e.g. Syrah) markedly decreases with increasing evaporative demand demonstrating low stomatal control over transpiration. In contrast the Ψ_{leaf} of isohydric cultivars (e.g. cultivar Grenache) remains stable with increasing evaporative demand demonstrating high stomatal regulation over transpiration (Guisard, 2008).

Typically, the diurnal course of leaf water potential shows large variability (Loveys, 2005). Jones (1990, 2007) reported on the rapid response by leaf water potential to environmental changes and therefore the difficulty of interpreting the measurements (see Figure 4).

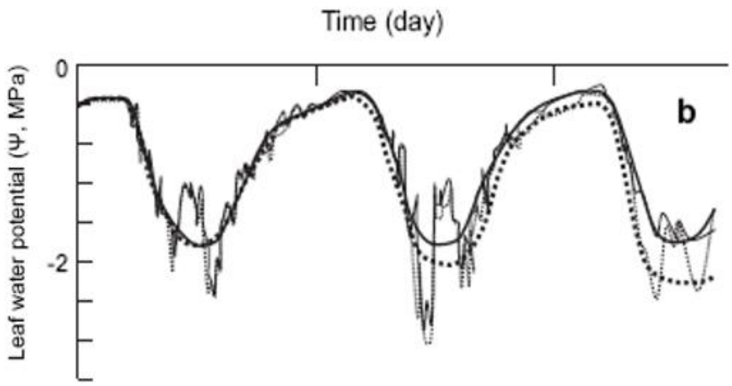

Figure 4 Illustration of the time course of leaf water potential over three days. Continuous lines represent the irrigated control; dashed lines represent a treatment where water is withheld at the start of the measurements. Smooth lines represent data smoothed using 3 hours running averages and oscillating lines represent instantaneous measurements. Reproduced from Jones (2007)

Reported threshold Ψ_{leaf} values for inducing stomatal control range between -1MPa (Carbonneau & Costanza, 2004; Williams & Trout, 2005) and -1.6MPa (Carbonneau et al. 2004; Schultz, 2003), with most accumulated around 1.3 to -1.45MPa (Freeman et al., 1982; M. Kliewer et al., 1983; Kriedemann & Smart, 1971).

<u>1.3.1.2 Pre-Dawn Leaf Water Potential</u>

Consecutively to the development of the pressure chamber (Scholander et al., 1965), pre-dawn leaf water potential (Ψ_{PD}) was measured in grapevines and various fruit trees (Klepper, 1968). This measure is now commonly accepted as an indicator of water stress (Carbonneau, 2004a, 2004b; Medrano et al., 2002). During the night, hydraulic gradients at the soil/root interface decrease and stabilise at a value related to the soil water content. The vine's hydraulic system equilibrates, and pre-dawn leaf water potential can be successfully used as a representative indicator of rootzone water status (Lebon et al., 2003).

1.3.1.3 Xylem (Stem) Water Potential

The assessment of water potential in shoot xylem Ψ_{xylem} is achieved from leaf petioles after the leaves have been covered and bagged for at least one hour. This allows the xylem water potential of the leaf petiole to equalise with that of the shoot (Chone, 2001). The use of xylem water potential (also termed stem water potential, Ψ_{stem}) over leaf water potential is based on a stronger correlation with transpiration in cases of mild water stress (Guisard, 2008).

Such estimates are also less variable than those of Ψ_{leaf} (Chone et al., 2000, 2001; Lopes et al., 1999).

Table 2 compares the threshold values of the various expressions of energy status (Ψ_{PD}, Ψ_{leaf} and Ψ_{xylem}) as reported in the literature.

Table 2 Summary of thresholds for various plant water potentials. Modified from Ojeda (2007), Williams and Araujo (2002) and Carbonneau (2002)

Stress intensity	Ψ_{PD} (MPa)	Ψ_{leaf} (MPa)	Ψ_{xylem} (MPa)
Mild	0.4	0.8	1.1
High	0.6	1.1	1.4
Severe	0.8	1.4	1.6

1.3.2 Canopy Temperature

Water constantly evaporates from surfaces while consuming energy depending on air temperature, air humidity and air velocity above the surface. This energy sink is used by plants to regulate the temperatures of the leaf surface via stomatal conductance of water vapour. Solving the leaf surface energy balance for leaf surface temperature has enabled researchers to formulate the hypothesis that if leaf temperature is known, the equation could be solved for stomatal conductance. In this way leaf temperature might be used as a plant-based indicator of water loss. The temperature of leaves with fully open stomata is below air temperature and increases above air temperature as stomata close (Campbell & Norman, 1998; Jones, 1992).

With the development of portable radiometer application in the field became more convenient and led to successful attempts to predict water stress and the requirement for irrigation in cereals and field crops. Technologies can vary from hand held thermometers to airborne thermography.

The increase of leaf temperature evidences a physical change in stomatal opening regardless of the cause of the change (Cifre et al., 2005), which is not the case in the leaf water potential - stomatal conductance relationship. Grant et al., (2007) showed that canopy temperature was able to differentiate between well irrigated grapevines and vines submitted to deficit irrigation. Similarly, Gonzalez-Dugo et al., (2006) showed that leaf temperature variability within the field of view may be a more sensitive indicator of water stress than leaf temperature itself.

1.3.3 Summary and Conclusions

This section has described the various plant-based indicators available to growers for assessing water stress and planning further viticultural practices. VPD was included due to its relationship with plant transpiration.

The evaluation of plant water status using leaf and pre-dawn water potential represents a large fraction of the literature reflecting its relevance in understanding plant water relationships. However, the relationship between leaf water potential and stomatal conductance reflects differences in the level of stomatal control over water vapour losses at the time of measurement. Stomatal control is itself a genetic response to drought adaptation and demonstrates the necessity to qualify the water potential measurements with some complementary information for appropriate interpretation.

Canopy temperature seems potentially to be a most convenient and useful plant-based indicator of water stress. Like other methods standardisation to remove non-stress related influences will be required. This feature of the measurement in particular makes it appropriate for remote sensing applications as well as land-based measurements. The potential to continually represent canopy conductance and hence quantify irrigation requirements is an attractive application of this technology. In order to explore the capabilities of this indicator, indices of plant stress based upon the surface temperature of leaves are now reviewed.

1.4 Thermal Indices

Tanner (1963) predicted that using portable infrared thermometers with the development of portable infrared thermometers plant temperature, when compared to a well-watered plant or when related to air temperature could be used to study moisture stress (Guisard, 2008). In addition, the observed plant temperature is available as both qualitative and quantitative indicators of plant water regimes (Tanner, 1963).

The energy balance for a crop's surface is described by various authors (Campbell & Norman, 1998; Jones, 1992):

$$Rn = H + \lambda_E + G$$

(Equation 14)

where Rn is the net radiant heat flux density ($W.m^{-2}$)
G is the soil heat flux density ($W.m^{-2}$)
H is the sensible heat flux density ($W.m^{-2}$)
λ is the heat of vaporisation ($J.mol^{-1}$)
E is the transpiration rate ($mol.m^{-2}.-s^{-1}$)

G is usually assumed to be negligible (Campbell & Norman, 1998), therefore reducing Equation 15 to:

$$Rn = (H + \lambda E)$$

(Equation 15)

where E can be defined as:

$$E = gs\frac{VPW}{pa}$$

(Equation 16)

and H can be defined as:

$$H = 2\, c_p\, g_{Ha}\, (T_{leaf} - T_a)$$

(Equation 17)

where pa is the atmospheric pressure (kPa)
c_p = 29.3 is the specific heat of air at constant pressure ($J.mol^{-1}.°C^{-1}$)
g_{Ha} is the boundary layer conductance for heat ($mol.m^{-2}.s^{-1}$)
T_{leaf} is the surface temperature of a leaf (°C)
T_a is the ambient air temperature (°C)

Equation 15 shows that the incoming radiation Rn is the driving source of energy for the leaf system, and that energy can only be lost via transpiration (λE) or sensible heat (H). λ is considered constant (44.1 $kJ.mol^{-1}$ at 20°C) and E is controlled by stomatal conductance (Equation 17). Loss of energy (H) is a function of g_{Ha} and related to wind speed.

If stomata close when radiation is steady, λE is reduced resulting in an elevation of T_{leaf}. Although largely simplified, this analysis forms the mechanistic justification for the use of leaf temperature as an indicator of stomatal behaviour.

The following sections review various indices based upon the evaluation of canopy temperature.

1.4.1 Stress Degree Day

Irrigation scheduling based on the canopy to air temperature differential (δTc-a) and the volumetric soil water content has mostly occurred in the form of the stress degree day (SDD) method, originally proposed by Jackson, Reginato & Idso (1977):

$$SDD = \sum_{n=i}^{N} Tc - Ta$$

(Equation 18)

where T_c is the canopy temperature at 2 p.m. (°C)
T_a is the air temperature at 2 p.m. (°C)
i is the first day after irrigation
N is the number of days required for SDD to reach a set value

Irrigation is started as soon as SDD exceeds 0. It was reported to predict successfully the onset of water stress in grapevines when δT_c-T_a was larger than -2.5°C (Ezzahouani & Williams, 2007).

1.4.2 Crop Water Stress Index

Crop Water Stress Index (CWSI) is a widely used indicator that provides an estimate of crop water status with respect to minimum and maximum levels of stress that can occur due to availability or unavailability of water. CWSI can be estimated using the following equation:

$$CWSI = \frac{Tcanopy - Twet}{Tdry - Twet}$$

(Equation 19)

where T_{canopy} is the canopy surface temperature (°C)
T_{wet} is the leaf surface temperature of the moistened reference leaf (°C)
T_{dry} is the leaf surface temperature of the oiled reference leaf (°C)

In grapevines, when used concurrently with infrared thermography. CWSI was able to distinguish between irrigation treatments (Grant et al., 2007; Möller et al., 2007; Walker, 1993).

1.4.3 Jones Index or Stomatal Conductance Index (I_g)

Jones (1999a) proposed to solve the energy balance equation by using reference surfaces representing a non-transpiring dry leaf (leaf coated with Vaseline) (T_{dry}, °C), and a 'pseudo' fully evaporating wet leaf surface (leaf sprayed with water) (T_{wet}, °C).

Combining a relative approach with a quantitative methodology, the energy balance (Equation 15) is solved for stomatal conductance (g_s) giving:

$$g_s = I_g \; x \; G$$

(Equation 20)

where

$$Ig = \frac{(Tdry - Tleaf)}{(Tleaf - Twet)}$$

(Equation 21)

1.4.4 Summary and Conclusions

This section reviewed the physiology of grapevines, in the context of water stress. It has been demonstrated that leaf and stem water potential measurements require expert interpretation with regard to providing information on stomatal and non-stomatal regulation of transpiration and CO_2 accumulation. These measures and Ψ_{PD} are nevertheless useful indicators of the water status of a grapevine.

Adaptive mechanisms to water stress were reviewed from a botanical aspect, describing the mechanisms of stomatal regulation. Several plant-based indicators of water stress were reviewed, and all were found to have various levels of suitability. Water potential (as leaf, pre-dawn or xylem) is by far the most used methodology for commercial.

Canopy temperature was shown to be correlated with the physical behaviour of stomata. Various indices based upon the temperature of canopies were reviewed and only indices derived from mechanistic methodologies (CWSI and I_g) were found to appropriately represent the situation of mild water stress. So far, the literature reviewed the assessment of grapevine indicating water stress. Central to that research is an appropriate technology to measure rapidly, accurately and cost effectively the variability of stomatal behaviour and its consequences in field grown grapevines.

In the following section the literature review will examine opportunities to provide an intercomparison of technology to monitor plant water status and detect the early onset of water stress using land based remotely sensed thermal imagery whilst checking on their reliability by comparing plant physiological variables.

1.5 Technology in Precision Viticulture

1.5.1 State of the Art Review

Vineyards are characterized by a high heterogeneity due to the cultivation environment, such as soil characteristics, microclimate, seasonal weather and cropping practices.

This variability causes different vine physiological response, with direct consequences on grape quality. Therefore, vineyards require a specific and differentiated agronomic management to satisfy the real needs of the crop, in relation to the spatial variability within the vineyard.

The introduction of new technologies for supporting vineyard management allows to improve the efficiency and quality of production and. at the same time, reduces the environmental impact, such as energy, fertilizers, chemicals and labour costs. Recent technological developments have allowed useful tools helping to monitor and control of many aspects of vine growth. Remote and proximal sensing sensors become strong investigation instruments of the vineyard status, such as water and nutrient availability, plant health and pathogen attacks, or soil conditions to describe spatial variability (Matese et al., 2015).

This chapter of the literature review presents a review of technologies used in precision viticulture. It is divided in two main sections. The first one focuses on monitoring technologies, which is the basis of mapping spatial variability; the second part discusses thermography, the technology utilized to provide information on canopy temperature.

1.5.2 Monitoring Technologies

The primary objective of the monitoring process is acquisition of the maximum amount of georeferenced information within the vineyard. A wide range of sensors aiming to monitor different parameters that characterize the plant growth environment are employed in precision viticulture for remote and proximal monitoring of geolocated data. (Matese & Di Gennaro, 2015)

1.5.3 Remote Sensing

Remote sensing is the detection and monitoring of physical characteristics of an object or phenomenon without making physical contact with it but by measuring its reflected and emitted radiation at a distance from the targeted area. Thus, it is in contrast to on-site observation.

1.5.3.1 UAV

Unmanned aerial vehicles (UAV), or also commonly called 'drones' found their way into precision viticulture due to automation development. These fixed or rotary wing platforms can fly autonomously and be remote controlled at visual range by a pilot on the ground or fly autonomously to a user-defined set of programmed waypoints. These platforms can be equipped with a series of sensors, which allow a wide range of monitoring operations to be performed.

A special feature about mounted sensors on UAV is the high spatial resolution (up to centimetres), their flexibility and their monitoring speed. For these reasons, UAV are ideal in vineyards of medium to small size (1–10ha), especially in areas characterized by high fragmentation due to elevated heterogeneity. Limiting factors are the payload weight and their operating time.

1.5.3.2 Remote Sensing Sensors and Applications

Applications of remote sensing in precision viticulture are focused mainly on reflectance spectroscopy, an optical technique based on reflectance measurement of the incident electromagnetic radiation at different wavelengths, particularly in the visible region (400-700nm), near infrared (700-1.300nm), and thermal infrared (7.500-15.000nm). Different surface types such as water, bare ground and vegetation reflect radiation differently in various channels. Therefore, the spectral reflectance of a body, such as a crop or soil, is called the 'spectral signature', and is represented on an XY graph, with the reflectance value on the ordinate and the wavelength of the spectrum on the abscissa (Matese et al., 2015).

Common sensors detect alterations of transpiration or photosynthetic activity on the leaf surface by measuring remotely leaf temperature, which increases when water stress conditions occur, as stomata closes reducing the water loss and at the same time interrupts the cooling effect of transpiration. In addition, alterations in photosynthetic activity are linked to the nutritional status, health, and vigour of the plants, and can be detected with multispectral and hyperspectral sensors.

Leaf reflectance is influenced by various factors in specific regions of the spectra: within the visible spectrum by the photosynthetic pigments, such as chlorophyll and carotenoids; in the near infrared spectrum by the structure of the leaves (size and distribution of air and water within the canopy); and in the infrared spectrum by the presence of water and biochemical substances, such as lignin, cellulose, starch, protein, and nitrogen.

Satellite and aerial images are used to estimate spatial patterns in crops, using vegetation indices such as the NDVI, that in turn can be related with different factors, such as the LAI (leaf area index), the presence of nutrient deficiencies, water stress status, or health status. (Matese et al., 2015)

1.5.4 Proximal Sensing

Proximal sensing or ground sensing technologies are able to outflank the problem of environmental interaction such as cloud or wind due to their close proximity to the vine canopy reducing or eliminating reflectance interference. When coupled with a differential GPS, these ground sensors are able to deliver data of high spatial resolution that can be integrated with material delivery systems to facilitate real-time and variable rate applications. In addition, many tools are available for continuous measurements carried by moving vehicles or instruments for precise ground observations made by an operator.

1.5.5. Thermal Imaging

The measurement of leaf temperature by using thermal infrared (IR) sensing is primarily used to study plant water relations, and especially stomatal conductance. A major determinant of leaf temperature is the rate of evaporation or transpiration from the leaf. The cooling effect of transpiration arises because a substantial amount of energy (the latent heat of vaporisation, λ; $Jmol^{-1}$, equation 15) is required to convert each mole of liquid water to water vapour, and this energy is then taken away from the leaf in the evaporating water and, thus, cools it. (Jones, 2004)

In-field, the non-invasive assessment of grapevine water status and its variability within the vineyard is a valuable tool in precision viticulture. Correlation analyses between thermal indices and physiological parameters such as g_s and leaf water potential have been carried out in the field using non-destructive portable sensors in commercial vineyards providing strong correlation levels. The main advantages these methods have, is the easy implementation and processing and immediate response.

Application on larger scale has been introduced by aerial thermal imaging, that successfully covered large extensions of vineyard or mounting automatic acquisition systems in on-work agricultural vehicles.

1.5.5.1 Difficulties on Field-Scale

Though the potential of infrared imaging for detection of hydric stress has been highlighted there are some disadvantages and specific considerations that need to be taken into account, such as

(1) The Variation of Radiation

Of particular interest for the application of thermal imaging to phenotyping and irrigation studies is the sensitivity of T_{leaf} (or of I_g and other indices) to changes in stomatal conductance as a function of the expected variation due to environmental variables. Here, the thermal approach will be of little value where the environmentally caused variation in temperature is greater than the 'sensitivity', that is the range in temperature caused by a specified variation in conductance (Jones 1994). Nevertheless, by viewing an ensemble of leaves in a canopy, it may be possible to obtain a more robust estimate of the mean temperature (Jones et al. 2002).

(2) Leaf Temperature Variation as Function of Absorbed Radiation

A critical variable in equation 16 for stomatal resistance is the net radiation absorbed by the leaf or canopy. This is because the leaf temperature increases linearly as absorbed radiant energy increases (other factors being constant). Several studies have demonstrated that the range of leaf temperatures for individual leaves in a homogeneous grapevine canopy may vary when comparing leaves directly illuminated normal to the solar beam and those in shaded parts of the canopy (Jones et al. 2002; Leinonen & Jones 2004; Grant et al. 2007). The temperature of any leaf will also depend on the position in the canopy and its orientation as a result of the local variation in irradiance, due to canopy structure and due to mutual shading.

Thus, the radiant energy absorbed by different leaves at any one time may vary by up to an order of magnitude, with consequential substantial impacts on canopy temperature. (Jones et al., 2009)

Canopy growth and architecture can affect the amount of sun-exposed leaf material: high vigour canopies will present more shading and bigger canopies low vigour canopies have a higher gap fraction, which will result in more sun-exposed leaf material. (Fuentes et al., 2012)

(3) Inclusion of Non-Leaf Material in the Analysis

The incomplete ground cover may have implications for the airborne thermography measurements through the potential aggregation of crop canopy and the background soil temperatures, which in the case of dry soil is often warmer than the crop canopy.

In such cases, a pixel is likely to comprise both soil and plant canopy temperatures, thereby resulting in 'mixed pixels'. The presence of mixed pixels is likely to affect the observed temperature toward the soil background temperature (Jones & Sirault, 2014).

(4) Data Analysis

There is a certain difficulty in the analysis of large volumes of data, since every pixel from each image is effectively a temperature reading (usually 5 megapixels per image) (Wang et al., 2010). If done manually, however, the necessary image processing can be rather labour-intensive and may also be dependent on subjective image interpretation.

<u>1.5.5.2 Conclusions</u>

The review on thermal imaging presented here shows the enormous potential for the use of thermal sensing at a field scale for detecting differences in stomatal conductance as a measure of plant response to water deficit. Although thermal imaging does not directly measure stomatal conductance, in any given environment stomatal variation is the dominant cause of changes in canopy temperature (Jones, 2004). It has also been widely suggested that thermal imaging can be used as a component of a remote sensing system for diagnosing plant stresses.

2. Materials and Methods

2.1 Experimental Sites

The study was conducted during the 2017 growing season in a 1.5-ha vineyard of a commercial winery in the Colli Piacentini area, Italy. The experimental site located near Borgonovo Val Tidone in the North West of Emilia-Romagna (44°59'22.3"N 9°22'01.8"E, 273 m above sea level) consists of the cultivar 'Barbera'. The six-year-old vineyard was planted along East-West row orientation, at a spacing of 2.5 m x 1.2 m (between row and in-the-row spacing, respectively), and with a vertical shoot positioning training system. The slope of the experimental field was around 5 - 20% in the East-West direction. The soil is mostly of clay loam texture.

Figure 5 Experimental site with visible spatial variability

The climate at the site is temperately sub continental, with warm but humid summers and cold winters. Annual minimum and maximum mean air temperatures occur in January and July, with values of 1.8°C and 23.4°C. Rainfall occurs mainly in autumn, winter and spring, with a long-term annual average of 858 mm. The driest month is July, with low rainfall during that period (for example, less than 56 mm during the 2017 season). This site is not irrigated.

Meteorological data for the entire experimental period were provided by an automated weather station of project NutriVigna, located within the experimental vineyard. Observations of the respective week (7 days) before each campaign give information about prevailing water stress.

The period before the 3rd of July is characterized by a medium temperature of 21.9°C and a maximum mean temperature of 29.5°C. At the onset of the observed week, 6mm of precipitation occurred. During the flight campaign of the 3rd of July between 1pm and 2pm the medium air temperature was 30.6°C and the maximum mean temperature was 32.3°C.

The increase of medium day temperature during the week preceding the campaign date is documented and represents a rising potential of hydric stress.

The period before the 26th of July is characterized by a medium temperature of 24.9°C and a maximum mean temperature of 32.5°C. This means a respective increase of 3°C compared to the period before the 3rd of July. In the middle of that observed week also 6mm of precipitation occurred. During the flight campaign of the 26th of July between 1pm and 2pm the medium air temperature was 30.2°C and the maximum mean temperature 31.3°C. Also in the case of this observed period, the increase of mean daily temperature during the week until the campaign date is documented and represents a rising potential of hydric stress.

2.2 Experimental Design

For the assessment of plant water status variability by proximal and remote thermal imagery and its comparison to ground measurements two experimental campaigns, ground-truthing and the drone campaign to remotely sense canopy temperature, were conducted on the 3rd and 26th of July 2017. Based on a Normalized Difference Vegetation Index (NDVI) map of the experimental site's differing vigour zones, eight vines of low and eight vines of high vigour were chosen to perform ground measurements and to be targeted by remote sensing.
Later, vines' performances within those 'treatments' of low vigour (LV) and high vigour (HV) were statistically analysed. With regard to water availability and individual vigour presented by the NDVI map, the behaviour towards water stress was assessed.

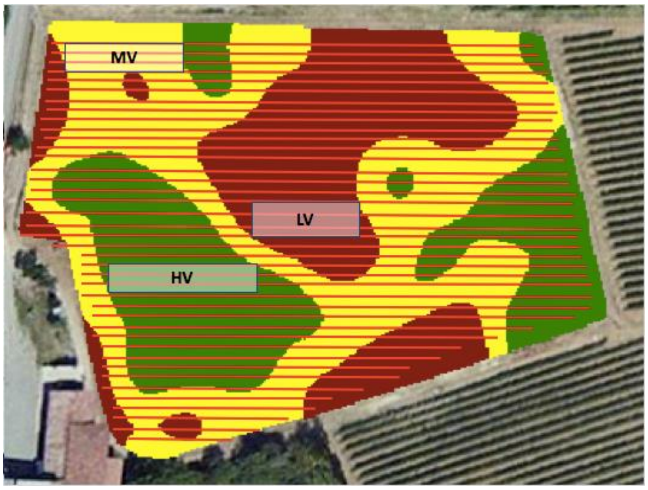

Figure 6 NDVI map presenting vigour zones and area of targeted vines

2.3 Plant Physiological Variables

2.3.1 Leaf Water Potentials

Vine water status by their leaf water potentials of four vines per vigour zone was evaluated on both experimental days using midday leaf water potential (Ψ_{MD}) measured by a Scholander pressure chamber (SKPM 1405, Skye Instruments Ltd, Llandrindod Wells, UK). Ψ_{MD} values were measured on two leaves per vine. The selected leaves were mature, healthy, and taken from the mid outer zone of the canopy. In addition, on the 26th of July 2017 predawn leaf water potential (Ψ_{PD}) was measured on four of eight vines per vigour zone, assumed to represent the mean soil water potential next to the roots. 2.3 Plant Physiological Variables

2.3.2 Leaf Gas Exchange

During Ψ_{MD} measurements, parameters of gas exchange, stomatal conductance (g_s), transpiration (E) and assimilation (A) were also measured on all tagged plants using a portable infrared gas analyser equipped with a leaf chamber having a window (LCi T Compact Photosynthesis System Hoddesdon, Herts, UK) on four fully-expanded and sun-exposed leaves (each with a basal, medium, apical and lateral leaf). Measurements were taken at ambient air temperature. The molar air flow rate inside the leaf chamber was 500 μmol.mol^{-1}. All measurements were taken at a reference CO_2 concentration similar to ambient (380 μmol.mol^{-1}) and at a saturating photosynthetic photon flux, ensuring that the leaves receive over 1000 μmol.m^{-2}.s^{-1} (no external light source was used in this study). The measurements for Ψ_{MD} were repeated for same plants; gas exchange for even the same leaves within each treatment. During both experimental campaigns, the plant-based variables were measured between 12:00 p.m. and 2:00 p.m. on the same day and time that the thermal images were acquired.

2.4 Soil Sampling

After the vegetative cycle, on the 26th and 28th of September 2017 in each targeted vigour zone three soil samples in the inner row were taken. The media of values for physical and chemical properties were presented and soil texture defined.

2.5 Thermal Imaging

2.5.1 Proximal Thermal Imaging

Proximal thermal imagery analysis was performed to support the results obtained from the UAV and plant physiological measurements. Single leaf temperatures of all targeted vines (basal, medium, apical and lateral leaves) and thermal measurements of both canopy sides (illuminated, south-facing and shaded, north-facing) were obtained using infrared thermography techniques by direct measurements performed during the experimental campaigns. Infrared images were taken using an infrared thermal imaging camera (FLIR i60).

The thermal resolution was 0.01°C and the accuracy of temperature measurement was less than ±2°C. Images were taken on sampling days, between 10.00 and 11.00 a.m., with a distance of 1.5m from the lateral canopy foliage. Canopy emissivity was set at 0.98. Visible digital images from the combined RGB acquisition imaging system of the camera were taken simultaneously with infrared measurements to support the subsequent analysis of the thermal images.

Wet and dry reference temperatures were also calculated on the 26th of July in line with the methodology mentioned in 1.4.3. For this, one leaf of each targeted plant was maintained continuously wet with cold water and photographed. It was used to estimate the reference wet temperature, and thus simulate leaves with fully open stomata. The reference dry temperature was estimated using Vaseline spread over the leaf's upper and lower surface. Here as well, an infrared camera picture was taken, and the recorded leaf temperature was used to estimate the reference dry temperature, and thus to simulate leaves with fully closed stomata. The two references were used in conjunction with canopy temperatures to calculate the linear thermal index (I_g) using equation 21.

2.5.1.1 Proximal-Sensed Data Collection and Processing

The thermal images acquired by the handheld thermal camera FLIR i60 were elaborated using the company's software FLIR Tools. It is possible to measure temperatures on a spot or within an area. By applying a frame on the leaf's picture mean, maximal and minimal temperature within the form can be monitored. Numeric temperature values were extracted leaf by leaf and out of canopy zones and means calculated to describe the foliar surface temperature. The program allows creating PDF reports to display the thermal image and its measurements. Further, to derive stress indices, values of minimum, maximum and mean temperatures were calculated for each photo frame inside a region of interest (ROI) of the canopy or vine leaf.

2.5.2 Remote Thermal Imaging

2.5.2.1 UAV Platform and Payload

Remote aerial surveys were performed by using an open-source UAV platform consisting of a modified multi-rotor MikrokopterOktoXL (HiSystems GmbH, Moomerland, Germany). Autonomous flight is managed by an on-board navigation system, which consists of a GPS module (U-blox LEA-6S, U-blox AG, Thalwil, Switzerland) connected to a navigation board (Navy-Ctrl 2.0, HiSystems GmbH, Moomerland, Germany) and a flight control unit (Mikrokopter Flight Controller ME V2.1, HiSystems GmbH, Moomerland, Germany) controlling six brushless motors. Two communication systems consisting of a duplex transmitter at 2.4 GHz (Graupner, Kirchheim, Germany) and a WiFi module (Mikrokopter, HiSystems GmbH, Moomerland, Germany) at 2.4 GHz allow control of the UAV navigation and monitoring of flight parameters, while a WiFi module provides video data transmission at 5.8 GHz ensuring real-time image acquisition control by the ground operator. The flight planning was managed through Mikrokopter Tool software (V2.20, HiSystems GmbH, Moomerland, Germany), which allows a route of waypoints to be generated as a function of the sensor Field of View (FOV) required overlaps between images and ground resolution. A thermal camera (FLIR TAU II 320, FLIR Systems, Inc., Wilsonville, OR, USA) was used for thermal data acquisition. This sensor, optimized for UAV applications, is of minimal size (44.5mm x 44.5mm x 30.0mm) and weight (72g) and has 324 pixels x 256 pixels resolution. It is able to measure long wave radiation in the spectral range 7.5 - 13µm.

2.5.2.2 Flight Survey

The UAV flight campaign was conducted in the experimental vineyard on the 3rd and 26th of July 2017. To extract and elaborate canopy temperatures for targeted vines, their geo-position was assessed using white papers of 30x42cm in front of each corresponding canopy. Later, those papers were visible and thermally measurable in the orthomosaic map, location of the vines could be obtained, and canopy temperatures extracted.

UAV surveys were conducted by flying once at 70m above ground level at midday, obtaining 0.09m pixel ground image resolution. The thermal camera setting was chosen to acquire and store 20 images per second with fixed time exposure. The waypoint route was generated to obtain more than 80% overlap both among photos (forward overlap) and among flight lines (lateral overlap), in order to achieve the highest accuracy in the mosaicking elaboration step. The images were recorded during clear sky conditions.

2.5.2.3 Remotely-Sensed Data Collection and Processing

Each pixel in a thermal image corresponds to a temperature at a given time. The method used to extract canopy temperatures consists of selecting manually pure vine pixel. To extract corresponding values for each vine's canopy, the UAV picture is uploaded into MathWorks® Matlab. Its user-friendly interface allows zooming to specific regions of interest (ROI). As ground sample panels were used to recognize the vines' canopies to sample, they are used to facilitate the further extraction of pure pixels of interest.

Clicking on a ground sample panels while zooming on the picture to get a close-up view of the corresponding vine, displays the pixels' temperature of the panels spot. By commanding extraction of features in the individual images masked pixels are exported as numeric values into a text file (figure 7).

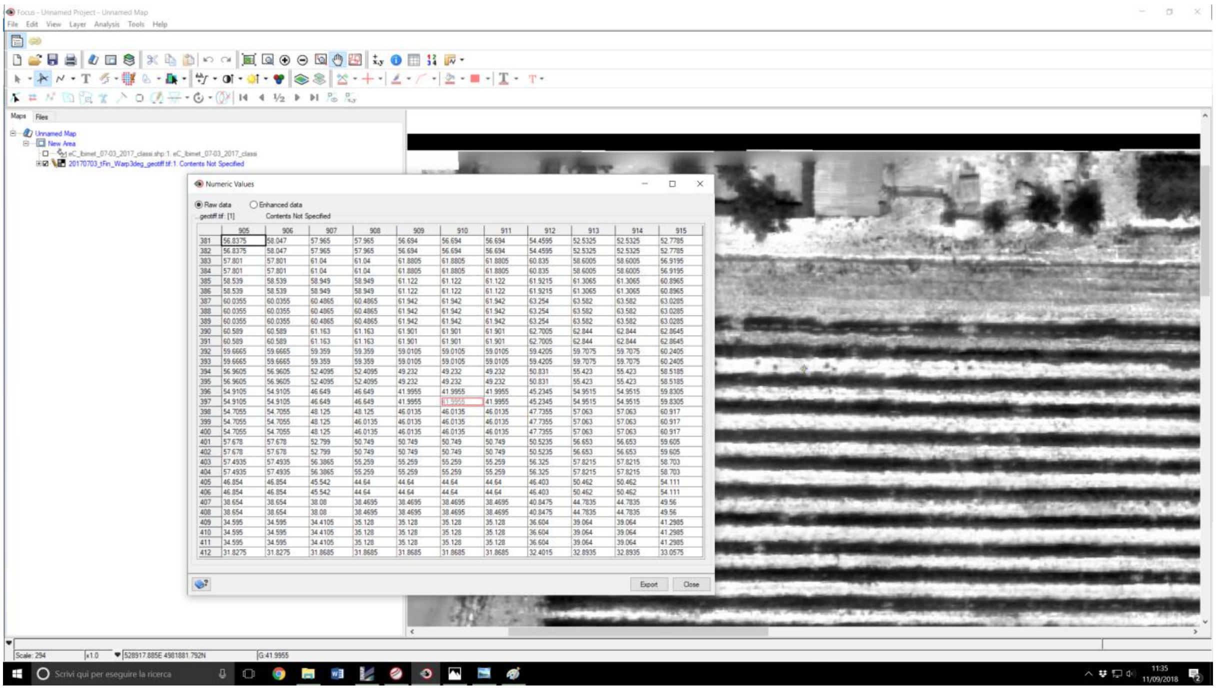

Figure 7 Numeric value extractions with Matlab. By targeting the ground sample panel surrounding pixel can be selected and transferred into Microsoft Excel for further elaboration.

Transforming them into a Microsoft Excel file, the cell representing the temperature of the previously marked spot of the ground sample panel is labeled with an asterisk within a map of computed pixel temperatures. The values are visually grouped by applying a coloured scale of green, red and yellow. By observing temperature groups and gradients, we are enabled to locate zones of different attributes (figure 8). While soil pixels represent high temperatures and are additionally coloured in shades of red, canopy pixels are aligned and represent a quite constant temperature.

As the ground sample panel's cell in excel is centered to a class of similar temperatures representing the whole surface of the panel, we can observe the thermal gradients above or below the panel, vertically upward or downward in the pixel map (depending on the vine's position from the ground sample panel) the expected cells related to the panel.

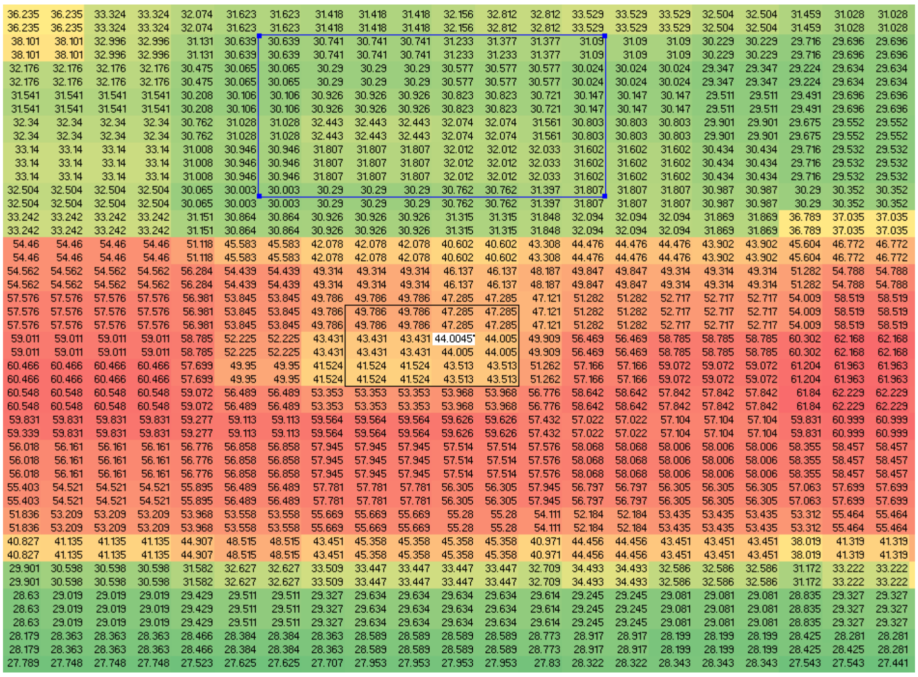

36.235	36.235	33.324	33.324	32.074	31.623	31.623	31.418	31.418	31.418	32.156	32.812	32.812	33.529	33.529	33.529	32.504	32.504	31.459	31.028	31.028
36.235	36.235	33.324	33.324	32.074	31.623	31.623	31.418	31.418	31.418	32.156	32.812	32.812	33.529	33.529	33.529	32.504	32.504	31.459	31.028	31.028
38.101	38.101	32.996	32.996	31.131	30.639	30.639	30.741	30.741	30.741	31.233	31.377	31.377	31.09	31.09	31.09	30.229	30.229	29.716	29.696	29.696
38.101	38.101	32.996	32.996	31.131	30.639	30.639	30.741	30.741	30.741	31.233	31.233	31.377	31.09	31.09	31.09	30.229	30.229	29.716	29.696	29.696
32.176	32.176	32.176	32.176	30.475	30.065	30.065	30.29	30.29	30.29	30.577	30.577	30.577	30.024	30.024	30.024	29.347	29.347	29.224	29.634	29.634
32.176	32.176	32.176	32.176	30.475	30.065	30.065	30.29	30.29	30.29	30.577	30.577	30.577	30.024	30.024	30.024	29.347	29.347	29.224	29.634	29.634
31.541	31.541	31.541	31.541	30.208	30.106	30.106	30.926	30.926	30.926	30.823	30.823	30.721	30.147	30.147	30.147	29.511	29.511	29.491	29.696	29.696
31.541	31.541	31.541	31.541	30.208	30.106	30.106	30.926	30.926	30.926	30.823	30.823	30.721	30.147	30.147	30.147	29.511	29.511	29.491	29.696	29.696
32.34	32.34	32.34	32.34	30.762	31.028	31.028	32.443	32.443	32.443	32.074	32.074	31.561	30.803	30.803	30.803	29.901	29.901	29.675	29.552	29.552
32.34	32.34	32.34	32.34	30.762	31.028	31.028	32.443	32.443	32.443	32.074	32.074	31.561	30.803	30.803	30.803	29.901	29.901	29.675	29.552	29.552
33.14	33.14	33.14	33.14	31.008	30.946	30.946	31.807	31.807	31.807	32.012	32.012	32.033	31.602	31.602	31.602	30.434	30.434	29.716	29.532	29.532
33.14	33.14	33.14	33.14	31.008	30.946	30.946	31.807	31.807	31.807	32.012	32.012	32.033	31.602	31.602	31.602	30.434	30.434	29.716	29.532	29.532
33.14	33.14	33.14	33.14	31.008	30.946	30.946	31.807	31.807	31.807	32.012	32.012	32.033	31.602	31.602	31.602	30.434	30.434	29.716	29.532	29.532
32.504	32.504	32.504	32.504	30.065	30.003	30.003	30.29	30.29	30.29	30.762	30.762	31.397	31.807	31.807	31.807	30.987	30.987	30.29	30.352	30.352
32.504	32.504	32.504	32.504	30.065	30.003	30.003	30.29	30.29	30.29	30.762	30.762	31.397	31.807	31.807	31.807	30.987	30.987	30.29	30.352	30.352
33.242	33.242	33.242	33.242	31.151	30.864	30.864	30.926	30.926	30.926	31.315	31.315	31.848	32.094	32.094	32.094	31.869	31.869	36.789	37.035	37.035
33.242	33.242	33.242	33.242	31.151	30.864	30.864	30.926	30.926	30.926	31.315	31.315	31.848	32.094	32.094	32.094	31.869	31.869	36.789	37.035	37.035
54.46	54.46	54.46	54.46	51.118	45.583	45.583	42.078	42.078	42.078	40.602	40.602	43.308	44.476	44.476	44.476	43.902	43.902	45.604	46.772	46.772
54.46	54.46	54.46	54.46	51.118	45.583	45.583	42.078	42.078	42.078	40.602	40.602	43.308	44.476	44.476	44.476	43.902	43.902	45.604	46.772	46.772
54.562	54.562	54.562	54.562	56.284	54.439	54.439	49.314	49.314	49.314	46.137	46.137	48.187	49.847	49.847	49.314	49.314	49.314	51.282	54.788	54.788
54.562	54.562	54.562	54.562	56.284	54.439	54.439	49.314	49.314	49.314	46.137	46.137	48.187	49.847	49.847	49.314	49.314	49.314	51.282	54.788	54.788
57.576	57.576	57.576	57.576	56.981	53.845	53.845	49.786	49.786	49.786	47.285	47.285	47.121	51.282	51.282	52.717	52.717	52.717	54.009	58.519	58.519
57.576	57.576	57.576	57.576	56.981	53.845	53.845	49.786	49.786	49.786	47.285	47.285	47.121	51.282	51.282	52.717	52.717	52.717	54.009	58.519	58.519
57.576	57.576	57.576	57.576	56.981	53.845	53.845	49.786	49.786	49.786	47.285	47.285	47.121	51.282	51.282	52.717	52.717	52.717	54.009	58.519	58.519
59.011	59.011	59.011	59.011	58.785	52.225	52.225	43.431	43.431	43.431	44.0045*	44.005	49.909	56.469	56.469	58.785	58.785	58.785	60.302	62.168	62.168
59.011	59.011	59.011	59.011	58.785	52.225	52.225	43.431	43.431	43.431	44.005	44.005	49.909	56.469	56.469	58.785	58.785	58.785	60.302	62.168	62.168
60.466	60.466	60.466	60.466	57.699	49.95	49.95	41.524	41.524	41.524	43.513	43.513	51.262	57.166	57.166	59.072	59.072	59.072	61.204	61.963	61.963
60.466	60.466	60.466	60.466	57.699	49.95	49.95	41.524	41.524	41.524	43.513	43.513	51.262	57.166	57.166	59.072	59.072	59.072	61.204	61.963	61.963
60.548	60.548	60.548	60.548	59.072	56.489	56.489	53.353	53.353	53.353	53.968	53.968	56.776	58.642	58.642	57.842	57.842	57.842	61.84	62.229	62.229
60.548	60.548	60.548	60.548	59.072	56.489	56.489	53.353	53.353	53.353	53.968	53.968	56.776	58.642	58.642	57.842	57.842	57.842	61.84	62.229	62.229
59.831	59.831	59.831	59.831	59.277	59.113	59.113	59.564	59.564	59.564	59.626	59.626	57.432	57.022	57.022	57.104	57.104	57.104	59.831	60.999	60.999
59.339	59.831	59.831	59.831	59.277	59.113	59.113	59.564	59.564	59.564	59.626	59.626	57.432	57.022	57.022	57.104	57.104	57.104	59.831	60.999	60.999
56.018	56.161	56.161	56.161	56.776	56.858	56.858	57.945	57.945	57.945	57.514	57.514	57.576	58.068	58.068	58.006	58.006	58.006	58.355	58.457	58.457
56.018	56.161	56.161	56.161	56.776	56.858	56.858	57.945	57.945	57.945	57.514	57.514	57.576	58.068	58.068	58.006	58.006	58.006	58.355	58.457	58.457
56.018	56.161	56.161	56.161	56.776	56.858	56.858	57.945	57.945	57.945	57.514	57.514	57.576	58.068	58.068	58.006	58.006	58.006	58.355	58.457	58.457
55.403	54.521	54.521	54.521	55.895	56.489	56.489	57.781	57.781	57.781	56.305	56.305	57.945	56.797	56.797	56.305	56.305	56.305	57.063	57.699	57.699
55.403	54.521	54.521	54.521	55.895	56.489	56.489	57.781	57.781	57.781	56.305	56.305	57.945	56.797	56.797	56.305	56.305	56.305	57.063	57.699	57.699
51.836	53.209	53.209	53.209	53.968	53.558	53.558	55.669	55.669	55.669	55.28	55.28	54.111	52.184	52.184	53.435	53.435	53.435	53.312	55.464	55.464
51.836	53.209	53.209	53.209	53.968	53.558	53.558	55.669	55.669	55.669	55.28	55.28	54.111	52.184	52.184	53.435	53.435	53.435	53.312	55.464	55.464
40.827	41.135	41.135	41.135	44.907	48.515	48.515	43.451	45.358	45.358	45.358	45.358	40.971	44.456	44.456	43.451	43.451	43.451	38.019	41.319	41.319
40.827	41.135	41.135	41.135	44.907	48.515	48.515	43.451	45.358	45.358	45.358	45.358	40.971	44.456	44.456	43.451	43.451	43.451	38.019	41.319	41.319
29.901	30.598	30.598	30.598	31.582	32.627	32.627	33.509	33.447	33.447	33.447	33.447	32.709	34.493	34.493	32.586	32.586	32.586	31.172	33.222	33.222
29.901	30.598	30.598	30.598	31.582	32.627	32.627	33.509	33.447	33.447	33.447	33.447	32.709	34.493	34.493	32.586	32.586	32.586	31.172	33.222	33.222
28.63	29.019	29.019	29.019	29.429	29.511	29.511	29.327	29.634	29.634	29.634	29.634	29.614	29.245	29.245	29.081	29.081	29.081	28.835	29.327	29.327
28.63	29.019	29.019	29.019	29.429	29.511	29.511	29.327	29.634	29.634	29.634	29.634	29.614	29.245	29.245	29.081	29.081	29.081	28.835	29.327	29.327
28.63	29.019	29.019	29.019	29.429	29.511	29.511	29.327	29.634	29.634	29.634	29.634	29.614	29.245	29.245	29.081	29.081	29.081	28.835	29.327	29.327
28.179	28.363	28.363	28.363	28.466	28.384	28.384	28.363	28.589	28.589	28.589	28.589	28.773	28.917	28.917	28.199	28.199	28.199	28.425	28.281	28.281
28.179	28.363	28.363	28.363	28.466	28.384	28.384	28.363	28.589	28.589	28.589	28.589	28.773	28.917	28.917	28.199	28.199	28.199	28.425	28.425	28.281
27.789	27.748	27.748	27.748	27.523	27.625	27.625	27.707	27.953	27.953	27.953	27.953	27.83	28.322	28.322	28.343	28.343	28.343	27.543	27.543	27.441

Figure 8 Temperature extractions of single pixels. Thermal data numeric values have been extracted from Matlab into Microsoft Excel and a colour scale has been applied. This case displays thermal gradients observed overhead, while concluding the position of the ground panels and hence, corresponding canopy.

Around the panel high temperatures connected to soil (coloured in shades of red) can be found, while further up and down moving to the suspected canopy in the pixel map displays decreasing temperature within a transition zone formed of soil pixels and canopy pixels (coloured in shades of yellow) until stable temperature is reached within a greater group of cells (shades of green). Very low temperatures within the map represent shade (coloured in darker green shades).

By selecting and marking several cells displaying an amount of pixel representing the vine's canopy and mindfully excluding temperatures that vary again, T for each plant is estimated by averaging values of pixels lying inside each intersected buffer. Based on a visual inspection of the mosaics, the pixel temperature ranges from between 27 and 34°C for corresponding vines.

2.6 Statistical Analysis

Differences between means of plant-based variables (g_s, A, E and Ψ_{MD}/ Ψ_{PD}) and thermal data in the vigour zones were assessed by one-way ANOVA using SSPS software (IBM SPSS Statistics), p-values less than 0.05 were taken to indicate statistically significant differences. Moreover, the evaluation included a linear regression analysis between plant-based variables and thermal data obtained from the sun exposed side of the canopy. The t-test to evaluate the null hypothesis was to intercept equal to zero and slope equal to unity at the 95% confidence level (i.e., $\alpha = 0.05$).

3. Results and Discussion

3.1 Vineyard Characterisation

Physiological data collection enables to characterise vineyard attributes and to get an idea of the physiological condition of the vigour zones in consideration of the fact of increasing water stress within the two field campaigns. The following chapter describes and discusses the collected various plant-based indicators to assess water stress. Additionally, the vineyard characterisation gets underpinned by pedologocal data.

3.1.1 Results of Soil Samples

Soil samples taken in the two vigour zones on the 26th and 28th of September were analysed for their physical and chemical properties. Results are presented in table 3. Figure 9 defines the soil texture in the soil texture triangle defined by the USDA.

Table 3 Physical and chemical soil characterisation of both vigour zones

	LV	Standard error LV	HV	Standard error HV
pH	8.3	0.02	8.2	0.01
Sand	45	0.58	26	0
Loam	27	0.67	30	0
Clay	28	0.88	44	0
$CaCO_3$ total	10	1	19.3	0.33
$CaCO_3$ active	5.0	0.19	10.9	0.23
Organic substances	1.09	0.02	1.55	0.03
N total	0.8	0.02	1.1	0.02
Ratio C/N	7.9	0.06	8.2	0.05
P assimilable	4.3	1.33	11.7	0.67
P_2O_5 assimilable	9.9	3.05	26.7	1.53
CEC	34.7	0.27	31.7	0.20
K ec	126.3	4.37	283.3	5.49
K_2O ec	151.6	5.25	340	6.58
Na ec	39.7	3.48	40.7	3.76
Ca ec	5343.3	130.72	5464.7	73.62
Mg ec	1251	52.37	801	25.81

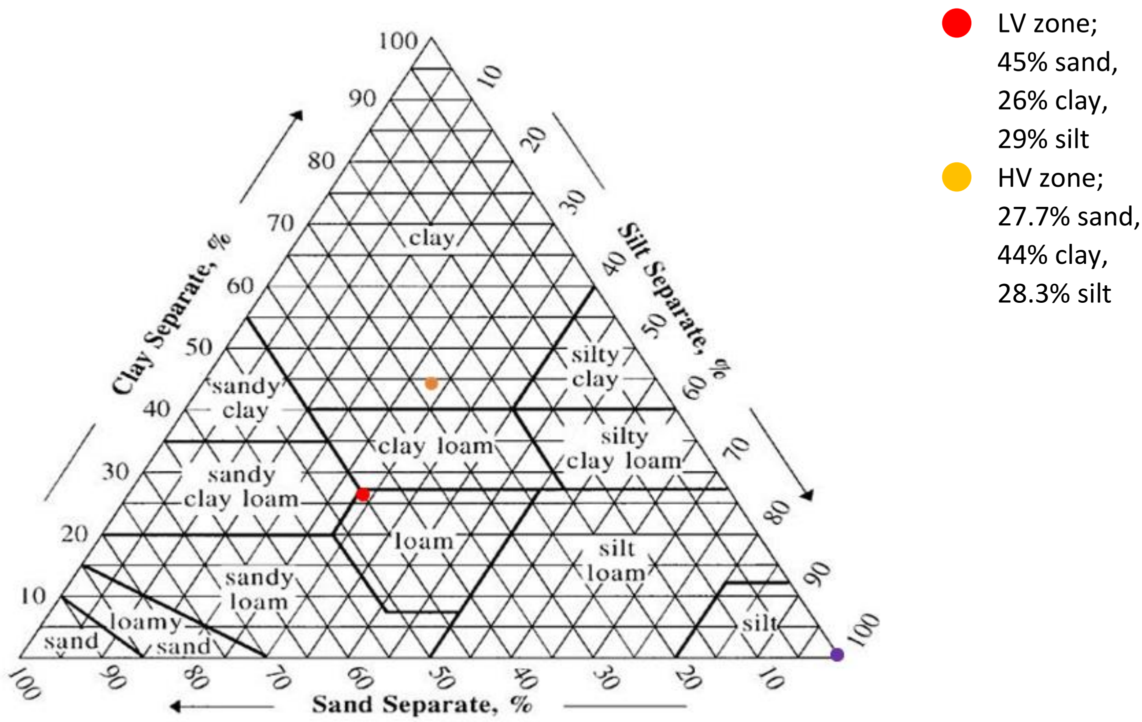

Figure 9 Soil texture triangle of the experimental site

If the soil water content becomes too low, plants become stressed. The plant available moisture storage capacity of a soil provides a buffer which determines a plant's capacity to withstand drought. The amount of water available to plants is therefore determined by the capillary porosity and is calculated by the difference in moisture content between field capacity and wilting point. This is the total available water storage of the soil.

In general, the higher the percentage of silt and clay sized particles, the higher the water holding capacity. Clay stores large amounts of water, but because it has a higher wilting point, it needs significant rain to be able to supply water to plants. On the other hand, sand has limited water storage capacity. Plants growing in sand generally have a denser root system to enable them to access water quickly before the sand dries out.

The two zones in which targeted plants got observed, show each pedologocal characteristics and potential water regimes related to the vigour zones determined by the NDVI assessment: Whilst the zone identified to be less vigorous has a higher percentage of sand, the more vigorous zone presents more clay. Plants response stated in vigour variability and plant physiological parameters root in the different soil characteristics

3.1.2 Characterisation of Vigour Zones by Plant Physiological Variables for the 3rd of July 2017

The collected data from the field campaigns are combined and presented in table 4 for the 3rd of July and table 6 for the 26th of July. Plant physiological variables were statistically examined for significant differences between the vigour zones.

Table 4: Leaf physiological traits and flux data recorded on 03.07.2017

Treatment	Ψ_{MD} (bar)	g_s (mol m^{-2} s^{-1})	E (mmol m^{-2} s^{-1})	A (µmol m^{-2} s^{-1})	WUE_{inst} A/E	WUE_i A/g_s
LV	- 10.4	0.101	5.219	6.933	1.352	69.189
HV	- 10.6	0.095	5.110	7.353	1.577	80.699
Significance	n.s.	n.s.	n.s.	n.s.	n.s.	n.s.

Significance codes for p-values: ns > 0.05

During the first field campaign on the 3rd of July no significant variation in any plant physiological variables between the treatments were found. Similar leaf water potentials occurred; both approaching a value of high water stress after table 2. Also similar stomatal conductance around 0.1 was observed, displaying a high impact by drought severity (table 1). However, those variances are merely displaying variability within leaf photosynthetic activity, but not giving an implementable model.

Knowing the severity of water stress by leaf water potentials, analysis of other predictors of water stress than vine water potential, was performed in the following; the best relationships between vine water status and other plant physiological variables in both vigour zones are presented.

When correlating leaf water potential with parameters describing leaf function, a strong statistical association occurs, represented by linear relationships. In detail, leaf water potential correlate with stomatal conductance for $y = -0.0178x + 0.2823$; $R^2 = 0.9305$ (figure 10), for net CO_2 assimilation rate $y = -0.8279x + 15.214$; $R^2 = 0.736$ (figure 11) and for transpiration rate $y = -0.9003x + 14.347$; $R^2 = 0.9112$ (figure 12).

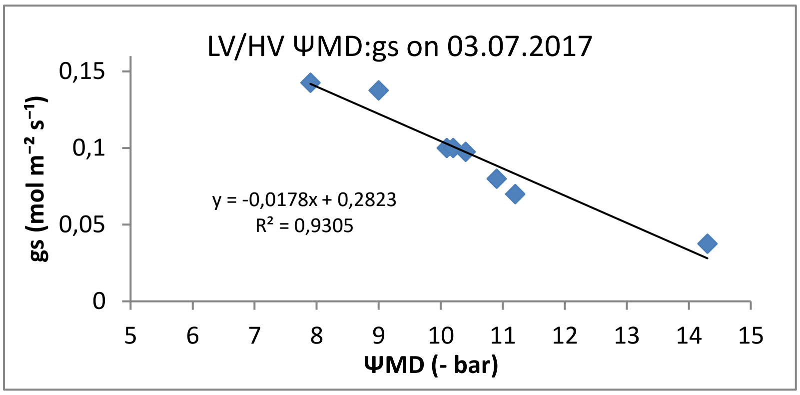

Figure 10 Correlation of midday leaf water potential and stomatal conductance on 03.07.2017 for the low and high vigour zone.

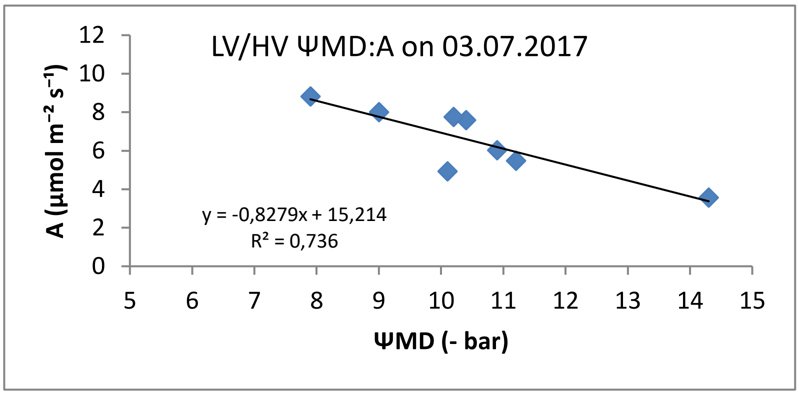

Figure 11 Correlation of midday leaf water potential and assimilation on 03.07.2017 for the low and high vigour zone.

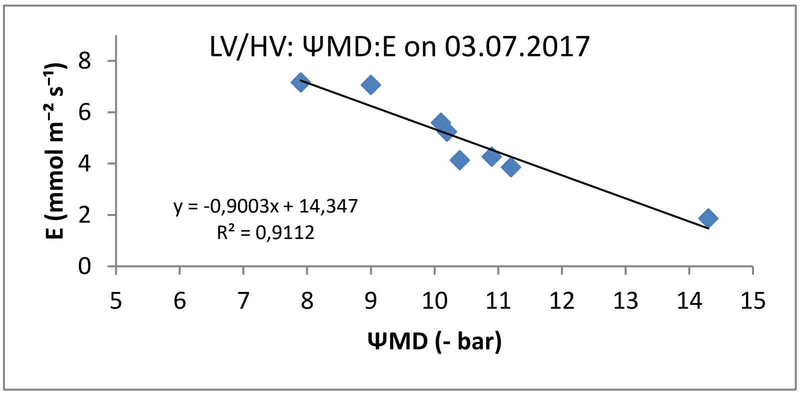

Figure 12 Correlation of midday leaf water potential and transpiration on 03.07.2017 for the low and high vigour zone

Therefore, those parameters appear to be valid to track water stress in grapevine, as the linear model explains not less than 73% of data variability. Additionally, a correlation of the atmospheric demand for water, the vapour pressure deficit (VPD) and transpiration (figure 13), was found ($y = 0.0029x - 10.847$; $R^2 = 0.7476$), displaying that transpiration linearly decreased under an increasing vapour pressure deficit.

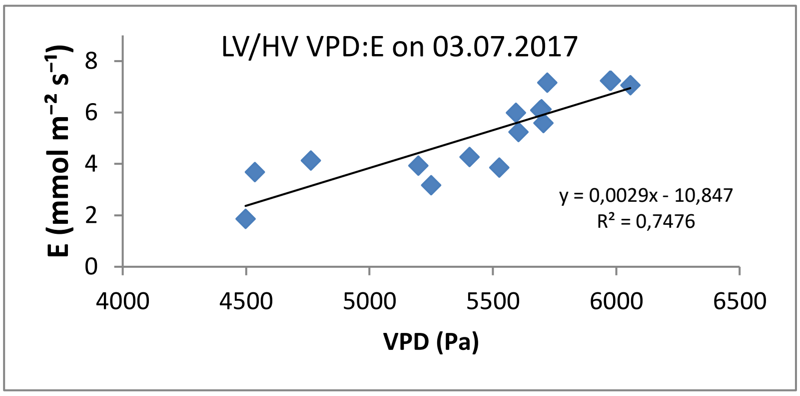

Figure 13 Correlation of vapour pressure deficit and transpiration on 03.07.2017 for the low and high vigour zone

3.1.3 Characterisation of Vigour Zones by Canopy Thermography for the 3rd of July 2017

The collected data from the field campaigns are presented in table 5 for the 3rd of July and in table 7 for the 26th of July. Thermal data were statistically examined for significant differences between the vigour zones at the two field campaigns.

Table 5: Single leaf and canopy (zone) temperatures recorded on 03.07.2017

Treatment	Canopy_N (C°)	Canopy_S (C°)	A.A._N (C°)	A.A._S (C°)	A.L._S (C°)	L.L._S (C°)	TD (C°)
LV	29.2	30.8	28.6	29.8	30.9	31.1	30.9
HV	29.0	31.1	28.4	30.2	32.2	31.0	28.6
Significance	n.s.	n.s.	n.s.	n.s.	n.s.	n.s.	***

Ground-based canopy temperature referred to: Canopy_N: North-facing side; Canopy_S: South-facing side; A.A._N: North-facing apical zone; A.A._S: South-facing apical zone; A.L._S: South-facing single apical leaves; L.L._S: South-facing lateral leaves. TD: Nadir-view canopy temperature taken by drone Significance codes for p-values: *** $p \leq 0.001$; ** $p \leq 0.01$; * $p \leq 0.05$; ns > 0.05

In accordance with the decrease in leaf water potential and stomatal conductance, the leaf and canopy temperature increase between the dates and also significant differences between the treatments are apparent.

At the first field campaign on the 3rd of July no significant thermal differences between the treatments can be detected by the thermal handheld camera. On the contrary, the thermal measurement by drone displays a significantly higher temperature of the LV canopy versus the HV canopy. This can be likely explained by the canopy shape and volume interactions within the two treatments. The canopy observed from overhead by the drone results in a nadir imaging. That means that a surface or a point is directly in line with the remote sensor. As a consequence, younger leaves, such as laterals and apical leaves in the apical canopy zone, with different photosynthetic capacity, get sensed. Crucial for the photosynthetic rate and therefore cooling by transpiration in LV, is the generally lower number of leaves in all leaf age classes, as the most important characteristic which is determining the reduction in the maximum CO_2 assimilated per vine. This significant difference, however, is not represented by measurements with the handheld camera. A possible explanation is a failure in data extraction, as the apical canopy zone with its apical shoots and leaves is discontinuously covered by leaf material. Therefore, also surroundings of the ROI were sensed and falsified, increased the temperature.

When correlating leaf water potential with canopy temperatures taken with the handheld camera, a strong statistical association occurs, sharing a linear relationship. In detail, leaf water potential measurements and simultaneous data collection of canopy temperature correlate for $y = 0.2234x + 28.674$; $R^2 = 0.7657$ (figure 14), especially in the HV zone for $y = 0.2213x + 28.787$, $R^2 = 0.9293$ (figure 15), while in the LV zone (figure 16) no correlation can be detected. A possible explanation for that phenomenon can be the fact of the comparatively low water stress of values between -10 and -11 bar for Ψ_{MD}. After table 2 and 1.3.1.1 were various thresholds for plant water status were repeated, only leaf water potential of -11bar and more negative is considered to represent high water stress. Therefore, a response in a rising leaf surface temperature is not compulsory measurable. In fact, this data is due to its small spread not sufficient to provide a compelling model.

Relating Ψ_{MD} with the canopy temperatures acquired by drone on the 3rd of July, the pairs of variables do not correlate strongly, however showing the same trend observed for Ψ_{MD} and temperatures acquired by the handheld camera. A possible explanation can be again the low variance between Ψ_{MD} displaying not even high water stress after table 2 and 1.3.1.1. Corresponding medium leaf temperature account for around 30°C, which is the upper limit of optimal leaf function reported in 1.2.3.

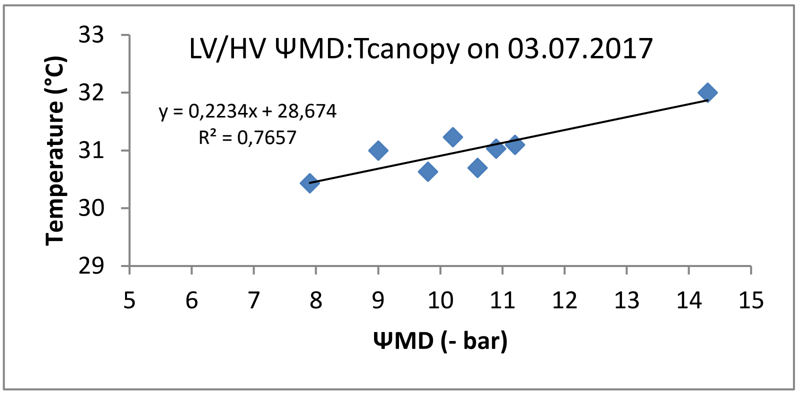

Figure 14 Correlation of midday leaf water potential and canopy temperature acquired by the thermal handheld camera on 03.07.2017 for the low and high vigour zone

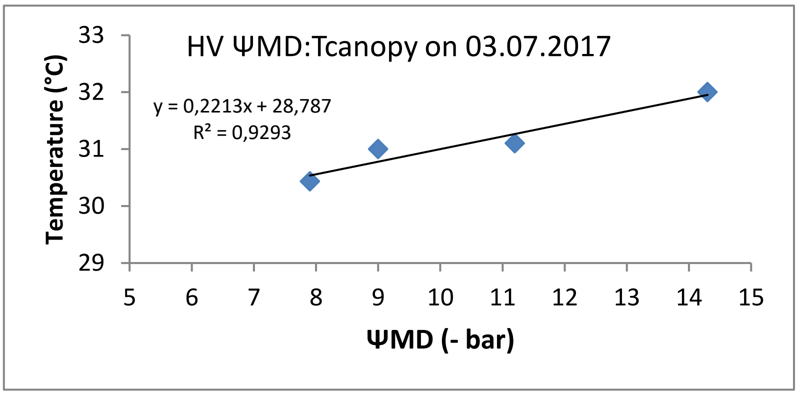

Figure 15 Correlation of midday leaf water potential and canopy temperature acquired by the thermal handhold camera on 03.07.2017 for the high vigour zone

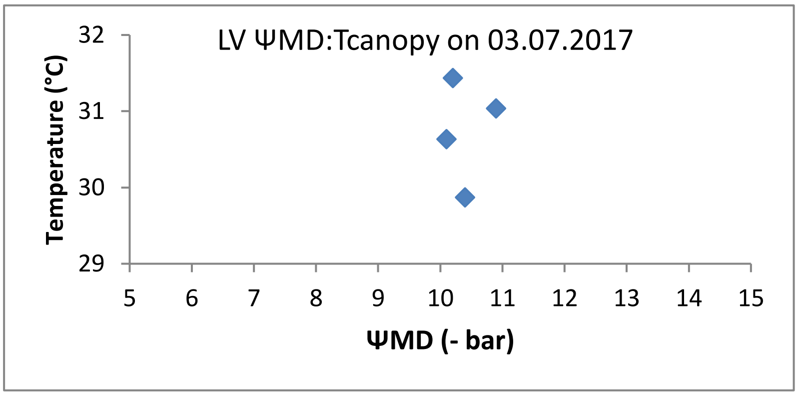

Figure 16 Non-correlation of midday leaf water potential and canopy temperature acquired by the thermal handhold camera on 03.07.2017 for the low vigour zone

As a consequence, canopy temperature appears to be valid to identify hydric stress in grapevine, as more than 76% of the data follow the linear relationship between vine water status and canopy temperature presented in the graphs.

3.1.4 Characterisation of Vigour Zones by Plant Physiological Variables for the 26th of July 2017

During the second field campaign on the 26th of July, beside the variable of Ψ_{MD}, no significant variation between the treatments were found (table 6). The Ψ_{MD} reflects a severe water stress for LV, same for the stomatal conductance within this zone; in contrast to HV where just a high severity for Ψ_{MD} and g_s (comparison table 1 and 2) is stated.

Table 6: Leaf physiological traits and flux data recorded on 26.07.2017

Treatment	Ψ_{PD} (bar)	Ψ_{MD} (bar)	g_s (mol m^{-2} s^{-1})	E (mmol m^{-2} s^{-1})	A (µmol m^{-2} s^{-1})	WUE_{inst} A/E	WUE_i A/g_s
LV	- 5.6	- 13.8	0.047	3.011	4.004	1.341	85.978
HV	- 4.0	- 11.0	0.064	3.399	5.542	1.596	89.418
Significance	n.s.	*	n.s.	n.s.	n.s.	n.s.	n.s.

Significance codes for p-values: *** p ≤ 0.001; ** p ≤ 0.01; * p ≤ 0.05; ns > 0.05

Same as for the previous date, no significant differences in photosynthetic activity between the vigour zones can be reported. However, comparing the shown data with the data in table 4, a decrease of all parameters is to observe; beside a stable instantaneous water use efficiency (WUE_{inst}), while between the two campaigns WUE_i increased about 25%, respectively 10% for each treatment, signalling the multiple environmental stimuli perceived and the ability of the plants within zones to sense the onset of changes in moisture availability and therefore modifies its water status as response improving WUE by restricted water consumption (Chaves et al., 2007; de Souza et al., 2005).

Between the two campaigns the targeted vines are presenting progressive signs of water stress illustrated by Ψ_{MD}: from an initiating high level on the 3rd of July to a high (in HV) respectively severe degree in LV on the 26th of July (comparison with table 2). This observation is underlined by the Ψ_{PD} measurements taken on the 26th displaying a mild to high water stress for HV and LV, respectively.

For HV it a less progressive decrease of Ψ_{MD} between the two dates is noticed, as the values have a similar mean variation at both field campaigns, whereas in LV the average Ψ_{MD} decreased around 25% at the 26th of July compared to the 3rd of July. This is when significant difference in that variable is spotted (table 6).

In the course of the 26th of July, beside midday water potential also the pre-dawn water potential of the targeted plants was recorded. Ψ_{PD} water potentials match in both cases with the following data collection of photosynthetic rates and present a regression line with a significant coefficient of determination for stomatal conductance g_s with y = -0.022x + 0.1638; R^2 = 0.9315 (figure 17), for net CO_2 assimilation rate y = -1.6827x + 13.15; R^2 = 0.8759 (figure 18) and for transpiration rate y = -0.6325x + 6.1137; R^2 = 0.7613 (figure 19) as functions of leaf water potential. Their negative correlation is sufficiently known from literature.

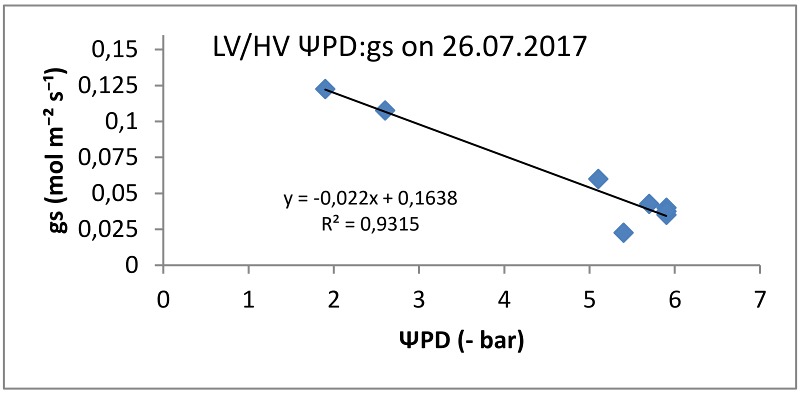

Figure 17 Correlation of pre-dawn leaf water potential and stomatal conductance on 26.07.2017 for the low and high vigour zone

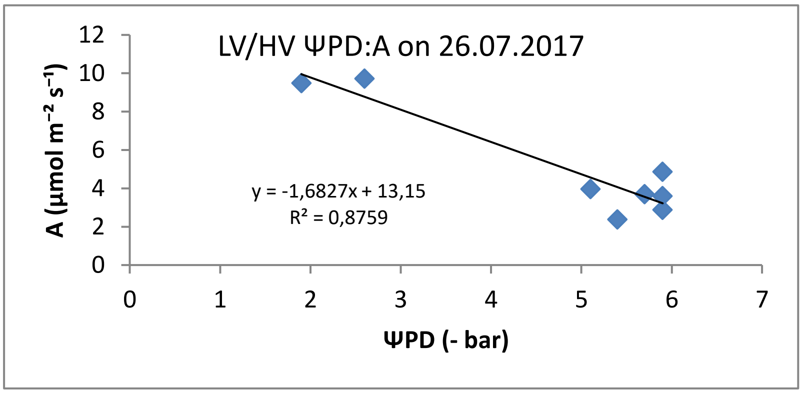

Figure 18 Correlation of pre-dawn leaf water potential and net carbon assimilation on 26.07.2017 for the low and high vigour zone

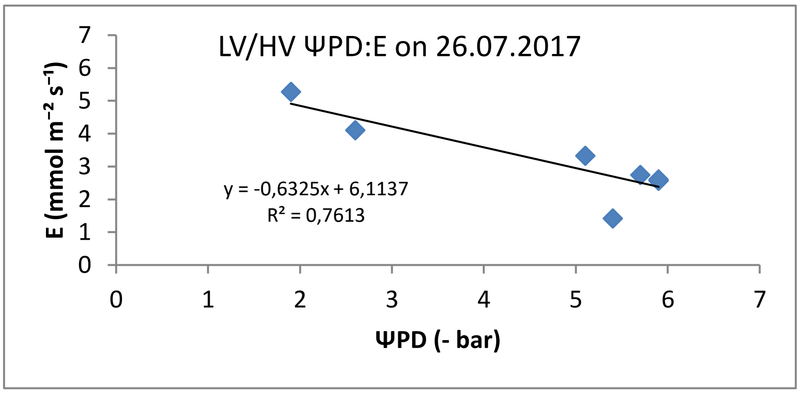

Figure 19 Correlation of pre-dawn leaf water potential and transpiration on 26.07.2017 for the low and high vigour zone

The same applies to the midday water potential and photosynthetic rate. Ψ_{MD} match in both cases with the measurements of photosynthetic activity and present a regression with a significant coefficient of determination for g_s with y = -0.0148x + 0.2416; R^2 = 0.7023 (figure 20), for net CO_2 assimilation rate y = -1.0877x + 18.574; R^2 = 0.6111 (figure 21) and for transpiration rate y = -0.4428x + 8.5735; R^2 = 0.6229 (figure 22) as functions of leaf water potential. Again, their negative correlation is expected and known from literature as mentioned in 1.2.6 as the vine water status is the driving force for stomatal mechanisms when a short-term adaption to drought events is necessary.

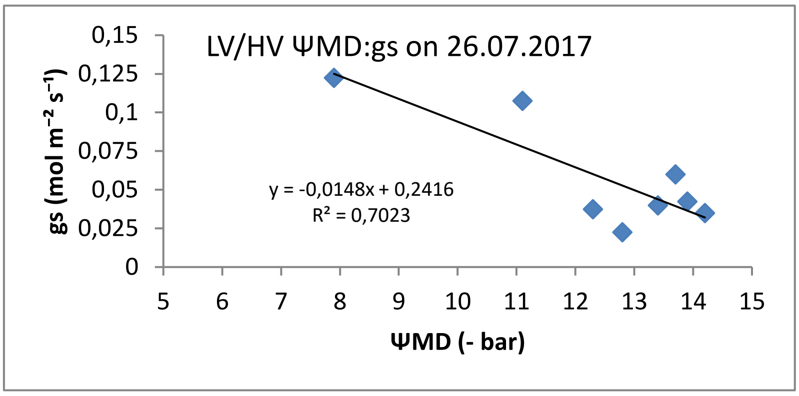

Figure 20 Correlation of midday leaf water potential and stomatal conductance on 26.07.2017 for the low and high vigour zone

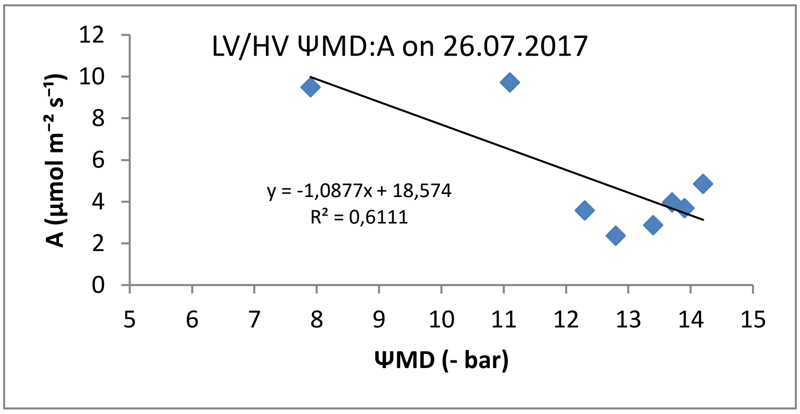

Figure 21 Correlation of midday leaf water potential and net carbon assimilation on 26.07.2017 for the low and high vigour zone

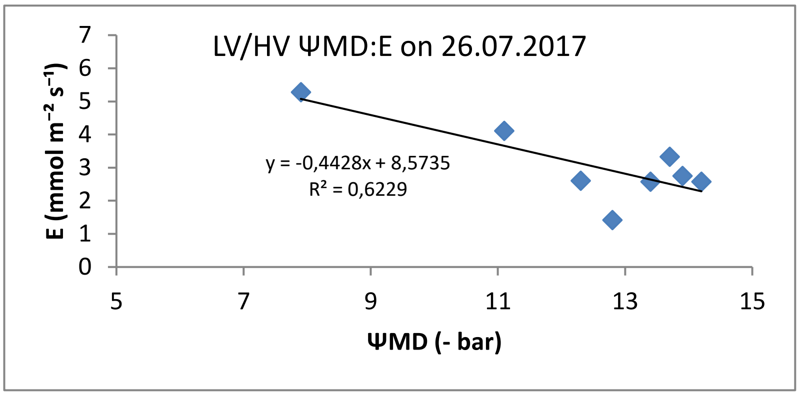

Figure 22 Correlation of midday leaf water potential and transpiration on 26.07.2017 for the low and high vigour zone

3.1.5 Characterisation of Vigour Zones by Thermography for the 26th of July 2017

Under on-going seasonal stress, the differential behaviour of the two vigour zones as related to different leaf and canopy temperature parameters is presented in table 7.

Table 7: Single leaf and canopy (zone) temperatures recorded on 26.07.2017

Treatment	Canopy_N (C°)	Canopy_S (C°)	A.A._N (C°)	A.A._S (C°)	A.L._S (C°)	L.L._S (C°)	TD (C°)
LV	30.238	31.621	28.638	30.412	30.487	29.835	33.350
HV	31.721	32.854	28.388	31.900	32.939	31.676	30.887
Significance	*	n.s.	n.s.	n.s.	*	*	**

Ground-based canopy temperature referred to: Canopy_N: North-facing side; Canopy_S: South-facing side; A.A._N: North-facing apical zone; A.A._S: South-facing apical zone; A.L._S: South-facing single apical leaves; L.L._S: South-facing lateral leaves. TD: Nadir-view canopy temperature taken by drone Significance codes for p-values: *** p ≤ 0.001; ** p ≤ 0.01; * p ≤ 0.05; ns > 0.05

From the first to the second field campaign an increase in single leaf and canopy (zone) temperatures is noted, due to the seasonal hydric stress.

The temperatures of the canopy sections differ significantly between the treatments: Temperatures extracted from thermal images taken of leaves or canopy sections with the thermal camera in HV are higher than respective measurements of LV. Especially highly located leaves, such as apical and lateral ones display a significantly higher surface temperature in HV, as they are less susceptible to mutual shading. Also on this date, the thermal measurement by drone displays a significantly higher temperature of LV canopy than of HV canopy, as observed and discussed for the 3rd of July in 3.1.2.

Correlating Ψ_{MD} with canopy temperatures measured by the handheld thermal camera, strong statistical association occurs, sharing a linear or polynomial relationship. In detail, leaf water potential measurements and simultaneous data collection for canopy temperature correlate for y = 0.324x + 28.583; R^2 = 0.8127 (figure 23), especially in the HV zone for a polynomial graph with y = 0.2175x^2 – 3.9096x + 48.473; R^2 = 0.9966 (figure 24). The same applies to the correlation of Ψ_{PD} and the proximally sensed canopy temperature with y = 0.4432x + 30.477; R^2 = 0.9109 (figure 25).

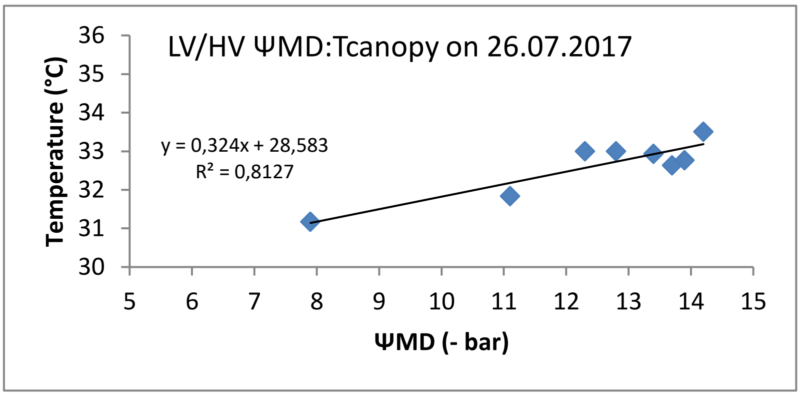

Figure 23 Correlation of midday leaf water potential and canopy temperature acquired by the thermal handheld camera on 26.07.2017 for the low and high vigour zone

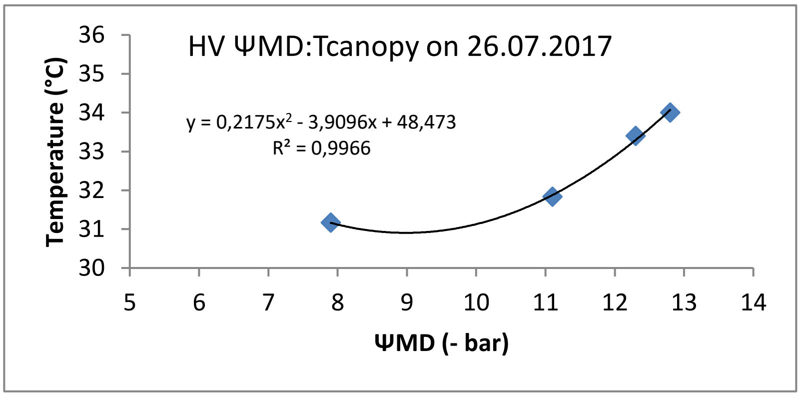

Figure 24 Correlation of midday leaf water potential and canopy temperature acquired by the thermal handheld camera on 26.07.2017 for the high vigour zone

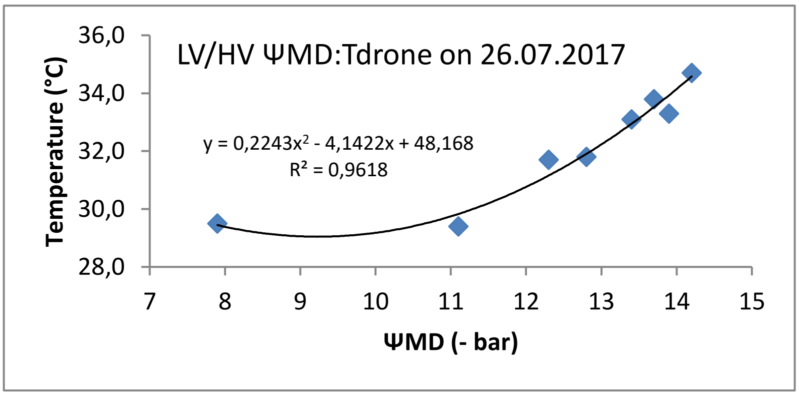

Figure 25 Correlation of midday leaf water potential and canopy temperature acquired by the drone on 26.07.2017 for the low and high vigour zone

When correlating Ψ_{MD} with canopy temperatures acquired by the drone, also here strong statistical correlation was present, sharing a linear or polynomial relationship. In detail, leaf water potential measurements and simultaneous data collection for canopy temperature correlate for $y = 0.2243x^2 - 4.1422x + 48.168$; $R^2 = 0.9618$ (figure 26). Correlating Ψ_{PD} with drone taken canopy temperatures, a linear relationship occurs, following $y = 1.0149x + 27.291$ with $R^2 = 0.7088$ (figure 27).

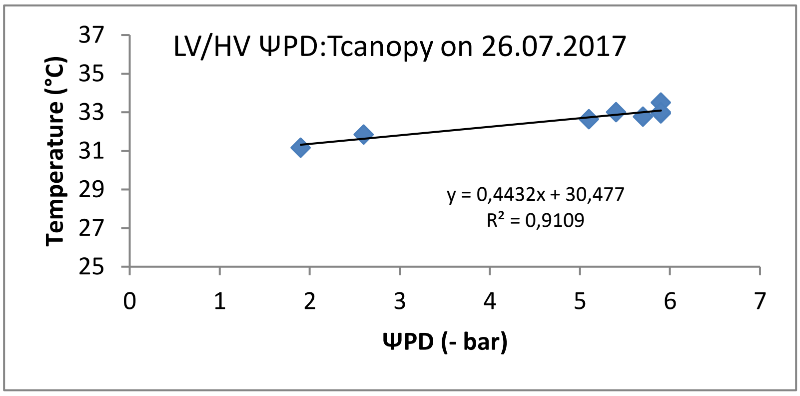

Figure 26 Correlation of pre-dawn leaf water potential and canopy temperature acquired by the handheld thermal camera 26.07.2017 for the low and high vigour zone

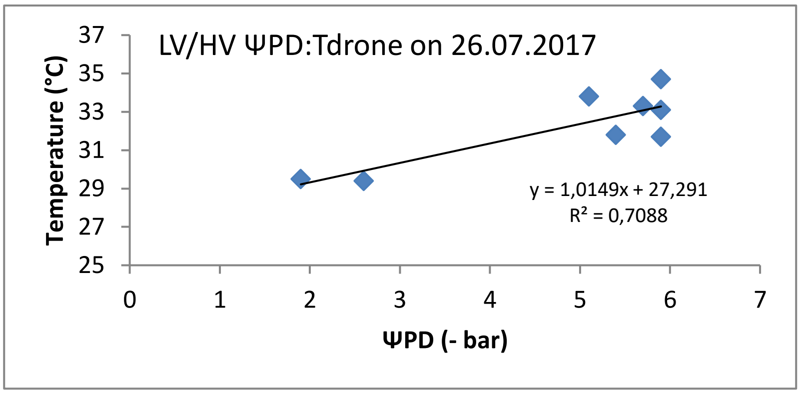

Figure 27 Correlation of pre-dawn leaf water potential and canopy temperature acquired by the drone on 26.07.2017 for the low and high vigour zone

Therefore, canopy temperature appears to be valid to identify hydric stress in grapevine, as data follow the linear relationship between vine water status and canopy temperature presented in the graphs.

3.2 Comparison of Thermal Data Assessment

The presented two methods for the assessment of plant water status by thermography were tested on the same plants and each of them shows correlations with ground measurements performed to evaluate plant physiological parameters. However, the absolute temperature differs from thermal handheld camera to the mounted thermal camera of the drone and the air temperature during the data acquisition. In the following, extracted values for the respective canopy by the two methods are visualized with reference to the air temperature and vine water status.

For the 3rd of July temperature estimation by drone of vines in HV zone is below canopy's temperature measured by the handheld thermal camera for a mean Δ 2.5°C (figure 28); just in the case of one plant, a fairly similar temperature results from the campaign. However, the temperature records' graphs follow in both cases of thermal data acquisition the same alternation as the plant water status for the four vines.

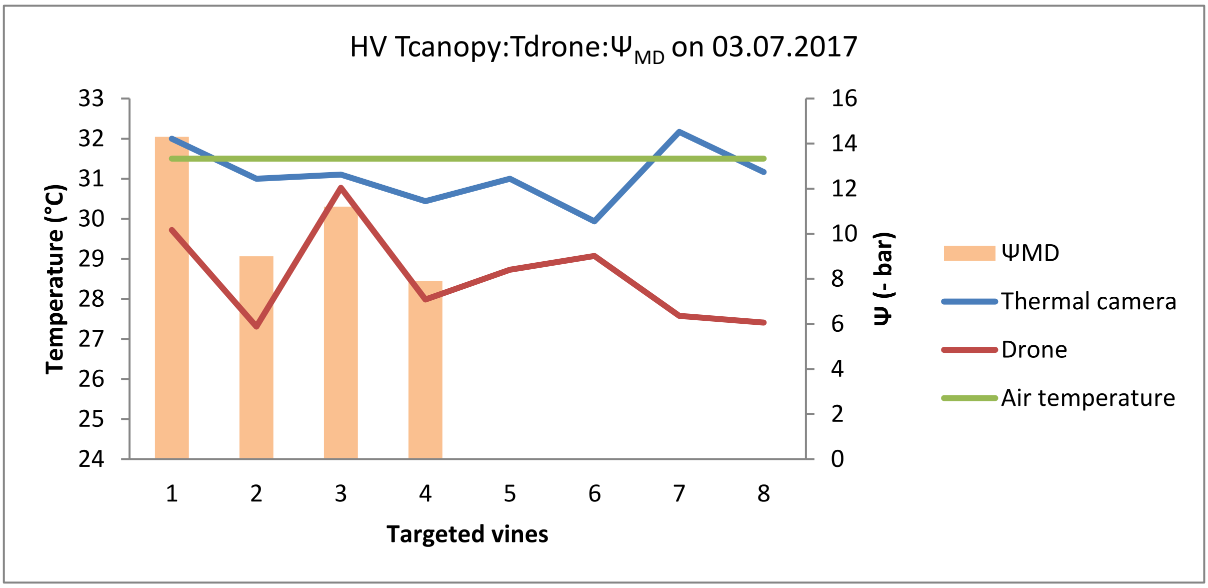

Figure 28 Comparison of thermal measurements and vine water status in the low vigour zone for the 03.07.2017

Conversely, in LV zone, curves are crossing and not harmonising their behaviour (figure 29). Measurements of both zones range most below the given air temperature (Tair) of 31.5°C, with Tdrone - Tair of a mean undercut of -2.3°C.

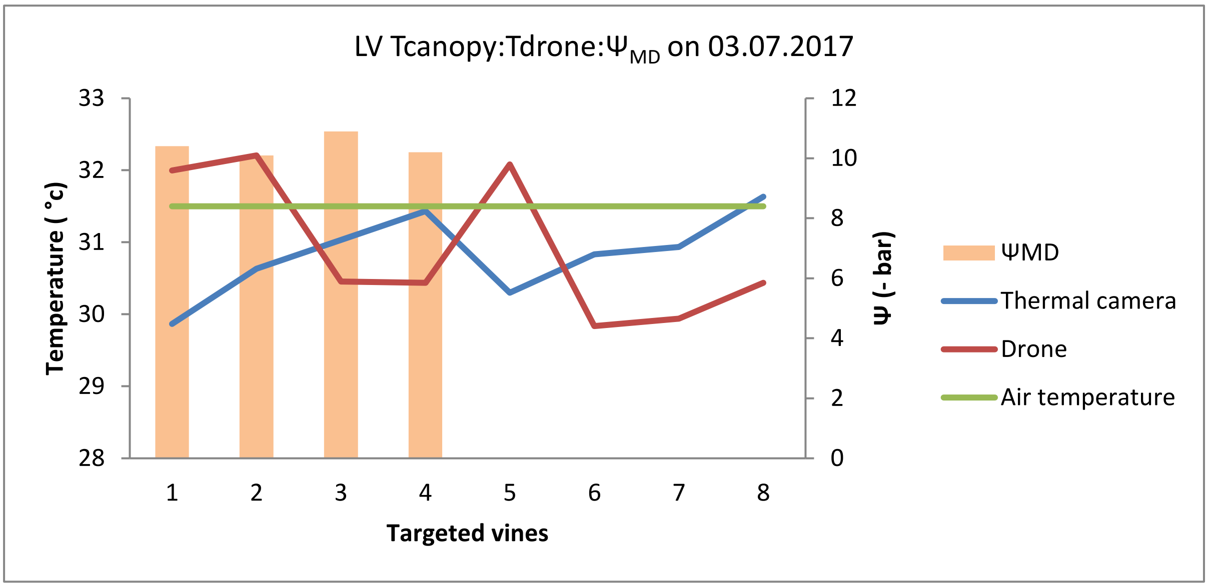

Figure 29 Comparison of thermal measurements and vine water status in the low vigour zone for 03.07.2017

The same phenomena of underestimation the canopy's temperature as in HV on the 3rd of July occurs for HV on the 26th of July for a mean Δ 2.0°C (figure 30). Again, for HV the temperature records' graphs follow in both cases of thermal data acquisition the same alternation as the plant water status (here Ψ_{MD} and Ψ_{PD}) for the four vines.

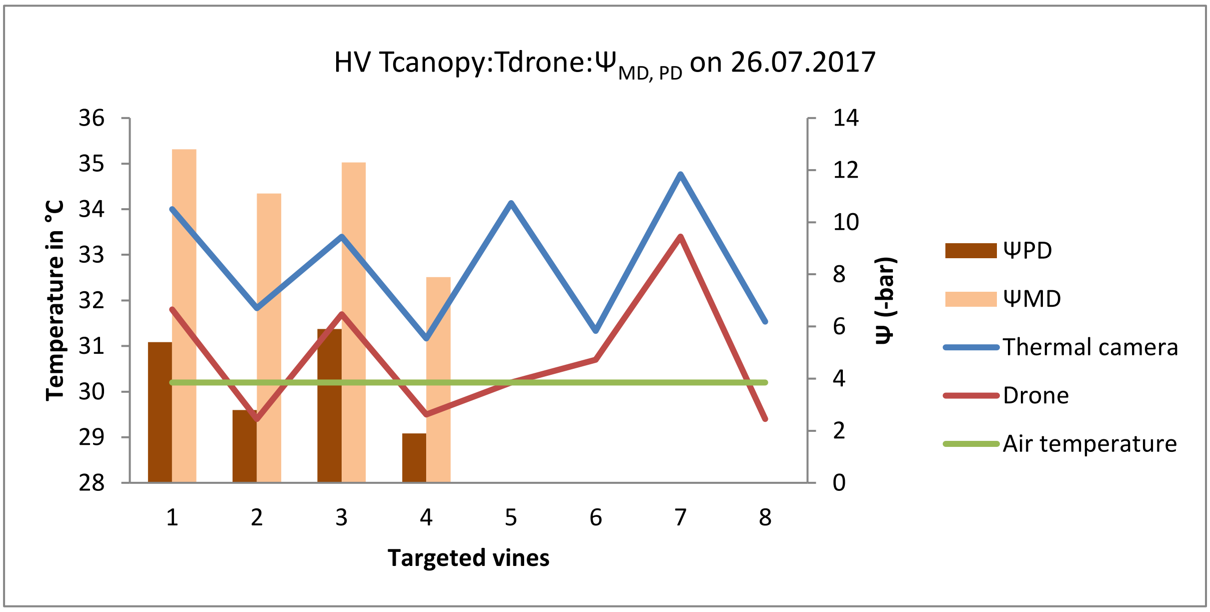

Figure 30 Comparison of thermal measurements and vine water status in the high vigour zone for 26.07.2017

In contrast to HV, in LV the drone's sensor is over-estimating canopy temperature for a mean Δ 1.7°C; however, the tendencies of the curves are similar (figure 31). Measurements of both treatments range most above the given air temperature of 30.2°C. Vine water status and graphs match to such a degree that no great up- and downturns occur. As Ψ_{PD} and Ψ_{MD} are not varying to greater extent between each other, also the graph does not respond with greater variation.

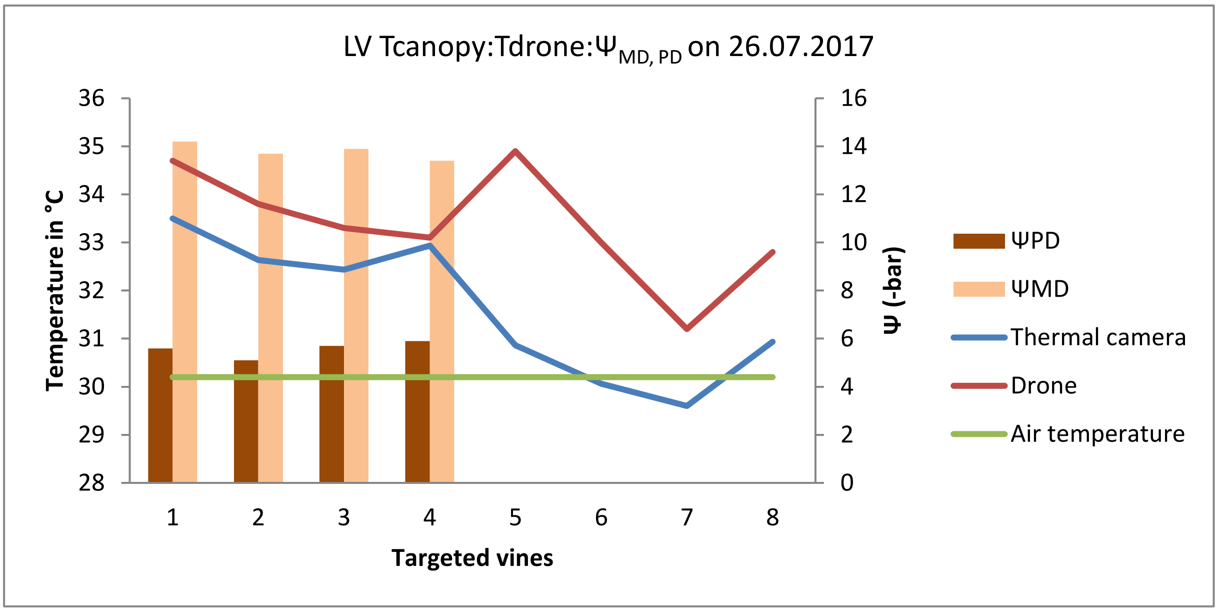

Figure 31 Comparison of thermal measurements and vine water status in the low vigour zone for 26.07.2017

Surveying the reproduced curves in this chapter, it is to examine that comparative measurements of both tools do not deliver a unitary leaf surface temperature for the canopy. As a consequence, the accuracy of the drone acquired thermal data and its reliability can be questioned when considering the proximal data from the handheld camera as a reference for leaf temperature. Several considerations can be applied.

A possible explanation complies with the fact, that the sensors are either exposed to a front view in the case of the handheld thermal camera or top view, as in the case of the drone's sensor. Therefore, different considerations regarding the ROI, the leaf surface, and external factors have to be done.

In the case of the proximal sensing by the handheld thermal camera, the canopy got sensed frontally from a short distance, when leaves are nearly vertically inclined. From that position also leaves of internal canopy layers, which are bedded behind the outer leaves and exposed to mutual shading, get sensed. In clearer canopies the opposite can be the case: if sensing in a low vigour canopy other material than leaves, air or soil can be sensed and falsify the data. As a consequence, during the temperature extraction from a thermal image showing a canopy front view, gaps and the clearer zone of lateral and apical leaves above the more continuous canopy have to be excluded. Therefore, the accurate separation of sunlit and shaded parts of a canopy by separating the required pixels from background and non-leaf material is necessary to provide more robust estimates (Leinonen et al., 2006, Möller et al., 2007).

In the case of thermal imaging by a drone, the sensors view is nadir, resulting in a perpendicular image of the canopy from top. Therefore, the ROI is the sun exposed canopy's crown, including especially apical and lateral leaves. Apical and lateral leaves show a seasonal course of net photosynthesis similar to the main leaves. Compared to the latter, especially laterals are formed later in the season, they are smaller and, due to their younger age; show a delayed senescence of 1-3 weeks and a higher net photosynthesis in the period following veraison. Apical and lateral leaves therefore make an important contribution to photosynthesis, therefore also to transpiration (Palliotti et al., 2018). When sensing the canopy crown, those leaves are measured in particular. Surveying the graphs displaying the comparative measurements in HV (figure 28 and 30), where a higher amount of foliar mass, apical and lateral leaves is given, it is to examine, that the temperatures acquired by drone are lower than the ones acquired by the handheld camera. This can be due to the fact that more photosynthetic active biomass and also mutual shading got sensed, while the proximal sensing also displays the naturally higher temperatures of older, basal and centered leaves. Observing the graphs for both methods in LV (figure 28 and figure 30), drone acquired temperature values are surmounting in most of the cases the proximal sensed temperature. Based on the previously presented fact of young vegetative growth having high photosynthetic activity (thus also transpiration), which is not given in a low vigour area, the higher temperatures measured by the drone compared to the temperatures acquired by the handheld camera can be explained by this.

Secondary, as presented already in the foregoing paragraph for proximal sensing, errors during data elaboration are possible, as data extraction out of the thermal image has to be limited to a narrow strip of pixels in a ROI. That results in a strict exclusion of pixels which are positioned at the edge of the canopy in the thermal picture.

Nevertheless, it could have occurred that mixel have been taken under consideration, rising the temperature due to soil interference. Conspicuous is the fact, that through all the correlations presented, the observations made for HV are showing closer relationships. This is complaisant to the hypothesis made, that the data extraction out of thermal images carries the risk of incorporating mixels and non-leaf material falsifying the values. That means, in HV the ROI is possibly better monitored by drone and handheld camera as the strip with single pixel can be clearly differed from a buffer zone suspected to be composed out of mixel and fewer gaps to sense are present. Thus, less mixel but more pure canopy pixels are in consideration of this data.

Likewise, another possible source of error in data acquisition beside the interference of non-leaf material pixels also environmental factors need to be considered. Wind speed should be taken into consideration and measured as close as possible to the targeted canopy, as it differs from wind speed usually measured by weather stations. Furthermore, canopies displaying a spherical leaf angle distribution typically exhibit a large degree of self-sheltering. Further studies should aim at better measuring or modelling wind speed spatially within the field of view of the thermographer, particularly when studies are carried out using airborne remote sensing (Guisard, 2008). Hence, weather fluctuations conditions such as change of global irradiation intensity, temperature, or wind speed must be much slower than the thermal time constant of the sensor during the whole flight campaign. A common environmental change that affects thermal imaging is clouds passing in front of the sun, which results in rapid changes of irradiance.

Visualizing the previous graphs of correlations and comparisons between the methods, it appears difficult to quantify a hydric stress by only observing single canopy temperatures. Particularly the likelihood that the variability in canopy temperature will increase with the stress severity, especially at locations with less available water, such as in LV, seems more difficult to conclude. Apparently, temperature measurements in LV seem to be distorted due to sensing of gaps and surroundings, as drone and handheld camera acquired data diverge. In HV on the contrary, a certain pattern of temperature variability as measured by plant physiological data can be detected and reconstructed by correlations. This, on account of more precise data acquisition due to minor inclusion of mixels and more significant variation in vine water potential. In addition, the second date of data acquisition, the 26th of July 2017, presents more significant correlations between parameters, especially vine water potentials, as values below -11 bar occurred, a threshold established signaling high water stress. Therefore, plant physiological parameters responded by displaying more significant differences between the zones furnished with different suspected water regimes.

Further, referring to 1.3.2, Gonzalez-Dugo et al., (2006) showed that leaf temperature variability within the field may be a more sensitive indicator of water stress than single leaf or canopy temperature itself. They state, that water stress amongst individual plants inevitably varies due to variations in factors such as soil properties, rooting depth and water availability. Therefore, spatial variability in the canopy temperature should be very low in the absence of water stress but should increase as the level of water stress increases. Thus, vine water stress is not only indicated by a higher canopy temperature in absolute values but is an implication of temperature variation within the field over time. As a consequence, a repetitive thermal data acquisition seems to be necessary to observe the spatial and seasonal variability of temperature.

4. Conclusions

Thermal imaging is a rapid and reliable method of measuring leaf surface temperatures. In-field, the non-invasive assessment of grapevine water status and its variability within the vineyard is a valuable tool in precision viticulture. Correlation analyses between thermal indices and physiological parameters such as g_s and leaf water potential have been carried out in the field using non-destructive portable sensors in commercial vineyards providing strong correlation levels. The main advantages these methods have, is the easy implementation and processing and immediate response. Therefore, the establishment of relationships between physiological parameters as photosynthetic rate and vines' water status presented provide a sound basis for determining the water use.

However, any study of physiological processes needs to take account of the temperature sensitivity of the process in relation to the likely natural variation (spatial and temporal) of temperature. The use of an absolute value of leaf temperature as an indicator of stomatal conductance or transpiration, however, is poorly meaningful by the fact that leaf temperature is also affected by a wide range of other plant and environmental characters according to the leaf energy balance and especially by the varying temperature figure due to the different optical imagining of the canopy. Furthermore, as the environment is constantly changing, at least for plants in the field, it also becomes necessary to consider the dynamic behaviour of leaf temperature in any precise study of leaf temperature.

Reference List

Aphalo, P. J., & Jarvis, J. A. (1991). Do stomata respond to relative humidity? Plant, Cell & Environment, 14, 127-132.

Baeza, P., Ruiz, C., Cuevas, E., Sotes, V., & Lissarrague, J. R. (2005). Eco-physiological and Agronomic Response of Tempranillo Grapevines to Four Training Systems. American Journal of Enology and Viticulture, 56 (2), 129-138.

Ball, J. T., Woodrow, I. E., & Berry, J. A. (1987). A model predicting stomatal conductance and its contribution to the control of photosynthesis under different environmental conditions. In J. Biggins (Ed.), Progress in Photosynthesis Research (Vol. 4, pp. 221-224). Dordrecht: M. Nijhoff.

Bellvert, J., Zarco-Tejada, P. J., Girona, J., & Fereres, E. (2014). Mapping crop water stress index in a ‘Pinot-noir’ vineyard: comparing ground measurements with thermal remote sensing imagery from an unmanned aerial vehicle. Precision agriculture, 15 (4), 361-376.

Bindi, M., Bellesi, S., Orlandini, S., Fibbi, L., Moriondo, M., & Sinclair, T. (2005). Influence of water deficit stress on leaf area development and transpiration of Sangiovese grapevines grown in pots. American Journal of Enology and Viticulture, 56 (1), 68-72.

Bravdo, B., Hepner, Y., Loigner, C., & Tabacman, H. (1985). Effect of crop level and crop load on growth, yield, must and wine composition and quality of Cabernet Sauvignon. American Journal of Enology and Viticulture, 36, 125-131.

Bunce, J. A. (1996). Does transpiration control stomatal responses to water vapour pressure deficit. Plant, Cell & Environment, 19, 131-135.

Campbell, G.S., & Norman, J. M. (1998). An introduction to environmental biophysics (2nd ed.): Springer.

Carbonneau, A. (2004a). Le raisonement de l'adaptation de la conduite du vignoble aux facteur climatiques. Paper presented at the Compte rendu technique Mondiaviti 2004, Bordeaux, France.

Carbonneau, A. (2004b). Qualité potentielle du raisin: base d'un modèle pratique d'evaluation. Journal International des Sciences de la Vigne et du Vin, 38 (1), 54-58.

Carbonneau, A., & Costanza, P. (2004). Response of vine leaf water potential to quick variation in canopy exposure. Example of canopy opening manipulation of Merlot (Vitis vinifera L.). Journal International des Sciences de la Vigne et du Vin, 38 (1), 27-33.

Chaerle L, Hagenbeek D, De Bruyne E, Valcke R, Van Der Straeten D. (2004) Thermal and chlorophyll-fluorescence imaging distinguish plant–pathogen interactions at an early stage. Plant & Cell Physiology 45, 887–896.

Chaves, M. M., Maroco, J. P. & Pereira, J. S. (2003). Understanding plant responses to drought - from genes to the whole plant. Functional Plant Biology, 30, 239-264.

Chaves, M. M., Pereira, J. S., Maroco, J., Rodrigues, M. L., Ricardo, C. P. P., Osorio, M. L., et al. (2002). How plants cope with water stress in the field. Photosynthesis and growth. Annals of Botany, 89, 907-916.

Chaves, M. M., Santos, T. P., Souza, C. D., Ortuño, M. F., Rodrigues, M. L., Lopes, C. M., ... & Pereira, J. S. (2007). Deficit irrigation in grapevine improves water-use efficiency while controlling vigour and production quality. Annals of Applied Biology, 150 (2), 237-252.

Chone, X. (2001). Contribution à l'étude des terroirs de Bordeaux: Etude des déficits hydriques modérés, de l'alimentation en azote et leurs effets sur le potentiel aromatique des raisins de Vitis vinifera L. cv Sauvignon Blanc. Doctoral Thesis. Université Victor Segalen Bordeaux 2.

Chone, X., Tregoat, O., & Van Leeuwen, C. (2001). Stem water potential is a better indicator than leaf water potential to survey and to manage field grown vine water deficits.

Chone, X., Tregoat, O., Van Leeuwen, C. & Dubourdieu, D. (2000). Vine water deficit: Among the 3 applications of pressure chamber, stem water potential is the most sensitive indicator. Journal International des Sciences de la Vigne et du Vin, 34 (4), 169-176.

Cifre, J., Bota, J., Escalona, J., Medrano, H., & Flexas, J. (2005). Physiological tools for irrigation scheduling in grapevine (Vitis vinifera L.). An open gate to improve water-use efficiency? Agriculture, Ecosystems and Environment, 105, 159-170.

Cruiziat, P., Cochard, H. & Ameglio, T. (2002). Hydraulic architecture of trees: main concepts and results. Annals of Forest Science, 59, 723-752.

Deery, D., Jimenez-Berni, J., Jones, H., Sirault, X., & Furbank, R. (2014). Proximal remote sensing buggies and potential applications for field-based phenotyping. Agronomy, 4(3), 349-379.

De Souza, C. R., Maroco, J. P., dos Santos, T. P., Rodrigues, M. L., Lopes, C., Pereira, J. S., & Chaves, M. M. (2005). Control of stomatal aperture and carbon uptake by deficit irrigation in two grapevine cultivars. Agriculture, Ecosystems & Environment, 106 (2-3), 261-274.

Deloire, A., Carbonneau, A., Wang, Z., & Ojeda, H. (2004). Vine and water, a short review. Journal International des Sciences de la Vigne et du Vin, 38 (1), 1-13.

Dixon, H. H., & Joly, J. (1895). On the ascent of sap. Philosophical Transactions of the Royal Society of London. B, 186, 563-576.

Düring, H. (2003). Stomatal and mesophyll conductance control CO_2 transfer to chloroplasts in leaves of grapevine (Vitis vinifera L.). Vitis, 42 (2), 65-68.

Escalona, J. M., Flexas, J., & Medrano, H. (1999). Stomatal and non-stomatal limitations of photosynthesis under water stress in field grown grapevines. Australian Journal of Plant Physiology, 26, 421-433.

Ezzahouani, A., & Williams, L. E. (2007). Effects of irrigation amount and preharvest irrigation cutoff date on vine water status and productivity of Danlas grapevines. American Journal of Enology and Viticulture, 58 (3), 333-340.

Farquhar, G. D., Ehleringer, J., & Hubick, K. T. (1989). Carbon isotope discrimination and photosynthesis. Annual Review of Plant Physiology and Plant Molecular Biology, 40, 503-537.

Ferrini, F., Matti, G. B., & Nicese, F. P. (1995). Effect of temperature on key physiological responses of grapevine leaf. American Journal of Enology and Viticulture, 46 (3), 375-379.

Fitzgerald, G. J., Rodriguez, D., Christensen, L. K., Belford, R., Sadras, V. O., & Clarke, T. R. (2006). Spectral and thermal sensing for nitrogen and water status in rainfed and irrigated wheat environments. Precision Agriculture, 7, 233-248.

Freeman, B. M., Kliewer, M., & Stern, P. (1982). Influence of windbreaks and climatic region on diurnal fluctuation of leaf water potential, stomatal conductance, and leaf temperature of grapevines. American Journal of Enology and Viticulture, 33 (4), 233-236.

Fuentes, S., De Bei, R., Pech, J., & Tyerman, S. (2012). Computational water stress indices obtained from thermal image analysis of grapevine canopies. Irrigation Science, 30 (6), 523-536.

Gaudillere, J. P., Van Leeuwen, C., & Ollat, N. (2002). Carbon isotope composition of sugars in grapevine, an integrated indicator of vineyard water status. Journal of Experimental Botany, 53 (369), 757-763.

Goldhamer, D., Fereres, E., Cohen, M., Girona, J., & Mata, M. (2000). Comparison of continuous and discrete plant-based monitoring for detecting tree water deficit and barriers to grower adoption for irrigation management. Paper presented at the Proceedings of the 3rd International Symposium on Irrigation of Horticultural Crops.

Gomez del Campo, M., Baeza, P., Riuz, C., & Lissarague, J. (2004). Water stress induced physiological changes in leaves of four container grown grape cultivars. Vitis, 43 (2), 99-105.

Gonzalez-Dugo, M. P., Moran, M. S., Mateos, L., & Bryant, R. B. (2006). Canopy temperature variability as an indicator of crop water stress severity. Irrigation Science, 24, 233-240.

Grant, O. M., Tronina, L., Jones, H. G., & Chaves, M. M. (2007). Exploring thermal imaging variables for the detection of stress responses in grapevine under different irrigation regimes. Journal of Experimental Botany, 58 (4), 815-825.

Guisard, Y. (2008). Crop Canopy Temperature as Indicator of Water Stress: Application to Grapevines (Doctoral dissertation, Charles Sturt University).

Idso, S. B. (1982). Non-water stressed baselines: A key to measuring and interpreting plant water stress. Agricultural meteorology, 27, 59-70.

Idso, S. B., Clawson, K. L., & Anderson, M. G. (1986). Foliage temperature: Effects of environmental factors with implications for plant water stress assessment and CO_2/climate connection. Water Resources Research, 22 (12), 1702-1716.

Idso, S. B., Jackson, R. D., Pinter Jr, P. J., & Reginato, R. J. (1981). Normalising the stress degree day parameter for environmental variability. Agricultural meteorology, 24, 45-55.

Jackson, R. D., Reginato, R. J., & Idso, S. B. (1977). Wheat canopy temperature: A practical tool for evaluating water requirements. Water Resources Research, 13 (3), 651-656.

Jacobs, C. M. J., van den Hurk, B. J. J. M., & de Bruin, H. A. R. (1996). Stomatal behaviour and photosynthetic rate of unstressed grapevines in semi-arid conditions. Agricultural and Forest Meteorology, 80, 111-134.

Jones, H. G. (1990). Physiological aspects of the control of water status in horticultural crops. HortScience, 25 (1), 19-26.

Jones, H. G. (1992). Plants and microclimate: a quantitative approach to environmental plant physiology (2nd ed.): Cambridge University Press.

Jones, H. G. (1998). Stomatal control of photosynthesis and transpiration. Journal of Experimental Botany, 49 (Special Issue), 387-398.

Jones, H. G. (1999a). Use of infrared thermometry for estimation of stomatal conductance as a possible aid to irrigation scheduling. Agricultural and Forest Meteorology, 95, 139-149.

Jones, H. G. (2004) Application of thermal imaging and infrared sensing in plant physiology and ecophysiology. Advances in Botanical Research 41, 107–163.

Jones, H. G. (2007). Monitoring plant and soil water status: established and novel methods revisited and their relevance to studies of drought tolerance. Journal of Experimental Botany, 58 (2), 119-130.

Jones, H. G., Serraj, R., Loveys, B. R., Xiong, L., Wheaton, A., & Price, A. H. (2009). Thermal infrared imaging of crop canopies for the remote diagnosis and quantification of plant responses to water stress in the field. Functional Plant Biology, 36 (11), 978-989.

Jones, H. G., Stoll, M., Santos, T., & de Sousa, C. (2002). Use of infrared thermography for monitoring stomatal closure in the field: application to grapevine. Journal of Experimental Botany, 53 (378), 2249-2260.

Klepper, B. (1968). Diurnal pattern of water potential in woody plants. Plant Physiology, 43, 1931-1934.

Kliewer, M., Freeman, B. M., & Hossom, C. (1983). Effect of irrigation, crop level and potassium fertilization on Carignan vines. Degree of water stress and effect on growth and yield. American Journal of Enology and Viticulture, 34 (3), 186-196.

Kriedemann, P. E. (1968). Photosynthesis in vine leaves as a function of light intensity, temperature and leaf age. Vitis, 7, 213-220.

Kriedemann, P. E., Kliewer, M., & Harris, J. M. (1970). Leaf age and photosynthesis in Vitis vinifera L. Vitis, 9, 97-104.

Le Clech, B. (1996). Fonctionnement hydrique de la vigne, de l'échelle de la journée à celle de l'année. Etude de quelques conséquences en viticulture. Université de Bordeaux 2, France.

Lebon, E., Dumas, V., Pieri, P., & Schultz, H. R. (2003). Modelling the seasonal dynamics of the soil water balance of vineyards. Functional Plant Biology, 30, 699-710.

Leinonen, L., & Jones, H. G. (2004). Combining thermal and visible imagery for estimating canopy temperature and identifying plant stress. Journal of Experimental Botany, 55 (401), 1423-1431.

Lenk S, Buschmann, C. (2006) Distribution of UV-shielding of the epidermis of sun and shade leaves of the beech (Fagus sylvatica L.) as monitored by multi-colour fluorescence imaging. Journal of Plant Physiology 163, 1273–1283.

Lopes, C. (1999). Relationship between leaf water potential and photosynthetic activity of filed grapevines under a Mediterranean environment. Paper presented at the 1st ISHS Workshop on Water Relations of Grapevines, Acta Horticulturae 493, Stuttgart, Germany.

Lopes, C., Vicente-Paulo, J., Pacheco, C., Tavares, S., Barraso, J., Rodrigues, M. L., et al. (1999). Relationship between leaf water potential and photosynthetic activity of field grapevines grown under different soil water regimes. Paper presented at the 11eme Journées GESCO - Groupe d'Etude des Systèmes de Conduite de la Vigne, Sicily, Italy.

Loveys, B. (2002). Physiological control of vine water use. Paper presented at the Vine and vineyard water requirements, Adelaide - Australia.

Loveys, B. (2005). When to water? Assessment of plant-based measurements to indicate irrigation requirements. Final report to the Grape and Wine Research and Development Corporation. (No. CSP02/02): CSIRO Plant Industry.

Lovisolo, C., & Schubert, A. (1998). Effect of water stress on vessel size and xylem hydraulic conductivity in Vitis vinifera L. Journal of Experimental Botany, 49 (321), 693-700.

Lu, P., Yunusa, I. A. M., Walker, R. R., & Muller, W. J. (2003). Regulation of canopy conductance and transpiration and their modelling in irrigated grapevines. Functional Plant Biology, 30, 689-698.

Matese, A., & Di Gennaro, S. F. (2015). Technology in precision viticulture: A state of the art review. International Journal of Wine Research, 7, 69-81.

Medrano, H., Escalona, J. M., Bota, J., Gulias, J., & Flexas, J. (2002). Regulation of photosynthesis of C3 plants in response to progressive drought: Stomatal conductance as a reference parameter. Annuals of Botany, 89, 895-905.

Monteith, J. L. (1995). A reinterpretation of stomatal responses to humidity. Plant, Cell & Environment, 18, 357-364.

Mott, K. A., & Parkhurst, D. F. (1991). Stomatal responses to humidity in air and helox. Plant, Cell & Environment, 14, 509-515.

Mullins, M. G., Bouquet, A., & Williams, L. E. (1992). Biology of the Grapevine (1st ed.). Cambridge, England: Cambridge University Press.

Ojeda, H. (2007). Irrigation qualitative de precision de la vigne (Qualitative precision irrigation in the vineyard). Progrès Agricole et Viticole, 124 (7), 133-141.

Palliotti, A., & Cartechini, A. (2001). Photosynthetic light response curves in relation to illumination of adaxial and abaxial surfaces of sun and shade leaves of Vitis vinifera L. Vitis, 40 (4), 175-177.

Palliotti, A., Cartechini, A. & Ferranti, F. (2000). Morpho-anatomical and physiological characteristics of primary and lateral shoot leaves of Cabernet Franc and Trebbiano Toscano grapevines under two irradiance regimes. American Journal of Enology and Viticulture, 51 (2), 122-130.

Palliotti, A., Poni, S. & Silvestroni, O. (2018). Manuale di Viticoltura. Milan, Italy: Edagricole-New Business Media

Poni, S., Intrieri, C., & Silvestroni, O. (1994). Interactions of leaf age, fruiting, and exogenous cytokinins in Sangiovese grapevines under non-irrigated conditions. I. Gas exchange. American Journal of Enology and Viticulture, 45 (1), 71-78.

Rodriguez, D., Sadras, V. O., Christensen, L. K., & Belford, R. (2005). Spatial assessment of the physiological status of wheat crops as affected by water and nitrogen supply using infrared thermal imagery. Australian Journal of Agricultural Research, 56, 983-993.

Sack, L., & Holbrook, M. N. (2006). Leaf hydraulics. Annual Review of Plant Biology, 57 (1), 361-381.

Salisbury, F. B., & Ross, C. W. (1992). Plant physiology (4th ed.). Belmont, California, USA: Wadsworth Publishing Company.

Scholander, P. F., Hammel, H. T., Bradstreet, E. D., & Hemmingen, E. A. (1965). Negative hydrostatic pressure can be measured in plants. Science, 148 (3668), 339-346.

Schultz, H. R. (2003). Differences in hydraulic architecture account for near-isohydric behaviour of two field grown Vitis vinifera L. cultivars during drought. Plant, Cell and Environment, 26, 1393-1405.

Schultz, H. R., Lebon, E., & Rousseau, C. (1999). Suitability of the "Ball, Woodrow, Berry" - model for the description of stomatal coupling to photosynthesis of different Vitis Species and Vitis vinifera cultivars in different climatic regions at various levels of water deficit.

Schultz, H. R., Pieri, P., Poni, S., & Lebon, E. (2001). Modelling water use and carbon assimilation of vineyards with different canopy structures and varietal strategies during water deficit. Paper presented at the 12th International Congress on Photosynthesis, Brisbane, Australia.

Slatyer, R. O., & Taylor, S. A. (1962). Terminology in soil-plant-water relations. Nature, 187, 922-924.

Stoll, M., & Jones, H. G. (2005). Infrared thermography as a viable tool for monitoring plant stress. Paper presented at the XIVth International GESCO Symposium, Geisenheim, Germany.

Tanner, C. B. (1963). Plant temperatures. Agronomy Journal, 55, 210-211.

Taylor, S. E. (1975). Optimal leaf form. In D. M. Gates & R. B. Schmerl (Eds.), Perspectives in biophysical ecology (pp. 609). New York: Springer-Verlag.

Ton, Y., & Kopyt, M. (2004a). Grapevine trunk and shoot diameter micro variations and trends as indicators of water potential. Paper presented at the 1st International Symposium on Grapevine Growing, Commerce and Research, Lisbon, Portugal

Tyree, M. T., & Ewers, F. W. (1991). The hydraulic architecture of trees and woody plants. New Phytologist, 119, 345-360.

Wang, X., Yang, W., Wheaton, A., Cooley, N., & Moran, B. (2010). Automated canopy temperature estimation via infrared thermography: A first step towards automated plant water stress monitoring. Computers and Electronics in Agriculture, 73 (1), 74-83.

Williams, L. E., & Baeza, P. (2007). Relationships among ambient temperature and vapor pressure deficit and leaf and stem water potentials of fully irrigated, field grown grapevines. American Journal of Enology and Viticulture, 58 (2), 173-181.

Williams, L. E., & Trout, T. J. (2005). Relationships among vine-and soil-based measures of water status in a Thompson Seedless vineyard in response to high-frequency drip irrigation. American Journal of Enology and Viticulture, 56(4), 357-366.

Wong, S. C., Cowan, I. R., & Farquhar, G. D. (1979). Stomatal conductance correlates with photosynthetic capacity. Nature, 282 (22nd November 1979), 424-426.

Appendix

Data Collection for 03.07.2017

		Proximal sensing single leaves: basal, media, alta, lateral											
Vigour	Plant	$\bar{x}$ Tmin basal	$\bar{x}$ Tmax basal	$\bar{x}$ Tmed basal	$\bar{x}$ Tmin media	$\bar{x}$ Tmax media	$\bar{x}$ Tmed media	$\bar{x}$ Tmin alta	$\bar{x}$ Tmax alta	$\bar{x}$ Tmed alta	$\bar{x}$ Tmin lateral	$\bar{x}$ Tmax lateral	$\bar{x}$ Tmed lateral
LV	P1	31.0	35.3	33.4	27.3	30.3	28.5	27.5	30.1	28.8	29.6	33.7	31.9
LV	P2	27.0	31.1	29.1	30.0	34.0	32.3	28.0	30.5	29.3	28.8	31.9	30.8
LV	P3	31.4	35.1	33.0	31.2	34.2	32.8	32.1	34.5	33.6	30.8	34.0	32.5
LV	P4	31.6	36.1	34.2	29.4	35.3	32.3	31.2	35.9	34.0	28.8	32.3	30.6
LV	P5	30.1	33.4	31.9	28.6	31.4	30.0	28.2	30.3	29.2	28.7	31.3	29.7
LV	P6	27.0	29.0	27.9	29.5	33.0	31.6	28.6	33.4	30.9	29.4	32.1	30.7
LV	P7	30.6	33.5	31.9	30.3	32.7	31.4	30.2	32.6	31.4	31.5	34.9	33.4
LV	P8	29.3	34.2	32.1	28.7	31.1	29.7	28.2	31.3	29.7	27.2	29.8	28.6
HV	P1	32.8	40.9	36.9	31.1	38.5	35.0	30.6	35.8	33.0	32.5	35.1	34.3
HV	P2	28.2	30.4	29.4	30.2	34.4	32.4	28.7	34.0	31.1	27.8	31.0	29.4
HV	P3	32.2	36.6	35.1	30.1	36.0	32.9	34.2	41.4	38.6	29.3	32.8	31.3
HV	P4	29.6	34.7	32.3	28.3	33.3	29.9	27.4	31.0	29.5	29.2	32.4	30.8
HV	P5	28.6	36.3	32.6	29.8	33.7	31.5	28.7	31.7	30.4	28.2	32.0	30.0
HV	P6	30.4	35.2	33.4	27.3	31.8	29.4	29.5	33.5	32.0	29.9	32.8	31.6
HV	P7	30.0	34.4	31.7	28.3	32.2	30.3	30.4	34.2	32.4	29.1	31.3	30.2
HV	P8	32.2	37.6	34.5	29.6	35.1	32.4	28.9	32.9	31.3	28.5	32.0	30.1

		Proximal sensing canopy (zones): South exposed, North exposed								
Vigour	Plant	Tmed S Canopy basal	Tmed S Canopy media	Tmed S Canopy alta	Tmax S Canopy alta	Tmed S Canopy	Tmed N Canopy basal	Tmed N Canopy media	Tmed N Canopy alta	Tmed N Canopy
LV	P1	31.7	29.4	28.5	31.3	29.9	30	28.5	28.3	28.9
LV	P2	32.2	30.4	29.3	33.3	30.6	30.4	29.2	28.3	29.3
LV	P3	32.1	31	30	33.9	31.0	30	29.1	29	29.4
LV	P4	32.8	30.8	30.7	34.9	31.4	30.3	28.7	28.6	29.2
LV	P5	32.1	29.7	29.1	33.3	30.3	28.1	27.5	27	27.5
LV	P6	31.5	30.9	30.1	36.7	30.8	30.9	30	30.1	30.3
LV	P7	32	31.1	29.7	35.4	30.9	29.7	29.5	28.8	29.3
LV	P8	32.8	31	31.1	39.2	31.6	30.2	29.5	29	29.6
HV	P1	33.1	31.8	31.1	35.2	32.0	30.6	29.3	29.3	29.7
HV	P2	33.2	30.3	29.5	36.5	31.0	29.5	28.2	28.1	28.6
HV	P3	31.9	30.7	30.7	33.4	31.1	30.7	29.7	29.4	29.9
HV	P4	33.5	28.9	28.9	37.2	30.4	30.6	27.9	27.1	28.5
HV	P5	31.4	30.7	30.9	36.5	31.0	29.4	28.6	28.8	28.9
HV	P6	31.1	29.9	28.8	34.9	29.9	28.6	27.2	27.1	27.6
HV	P7	33.8	31.3	31.4	40	32.2	30.7	29.3	28.6	29.5
HV	P8	32.4	30.6	30.5	36.6	31.2	30.4	29.1	28.7	29.4

		Remote sensing	Thermal data and comparisons			
Vigour	Plant	Drone	Tair	VPD	Tdrone - Tair	Tdrone - Tcanopy
LV	P1	32.0	31.5	2717	0.5	2.1
LV	P2	32.2	31.5	2773	0.7	1.6
LV	P3	30.5	31.5	2770	-1.0	-0.6
LV	P4	30.4	31.5	2723	-1.1	-1.0
LV	P5	32.1	31.5	2751	0.6	1.8
LV	P6	29.8	31.5	2691	-1.7	-1.0
LV	P7	29.9	31.5	2718	-1.6	-1.0
LV	P8	30.4	31.5	2769	-1.1	-1.2
HV	P1	29.7	31.5	2872	-1.8	-2.3
HV	P2	27.3	31.5	2956	-4.2	-3.7
HV	P3	30.8	31.5	3001	-0.7	-0.3
HV	P4	28.0	31.5	2946	-3.5	-2.4
HV	P5	28.7	31.5	3010	-2.8	-2.3
HV	P6	29.1	31.5	2978	-2.4	-0.9
HV	P7	27.6	31.5	3058	-3.9	-4.6
HV	P8	27.4	31.5	2932	-4.1	-3.8

	Plant physiological parameters						
Vigour	Plant	ΨMD	g_s	E	A	WUE A/E	WUE A/gs
LV	P1	10.4	0.0975	4.1275	7.5825	1.837	77.76923
LV	P2	10.1	0.1	5.585	4.9275	0.882274	49.275
LV	P3	10.9	0.08	4.265	6.035	1.415006	75.4375
LV	P4	10.2	0.1	5.2425	7.7575	1.479733	77.575
LV	P5		0.14	7.24	8.4575	1.168163	60.41071
LV	P6		0.0575	3.1725	4.1225	1.299448	71.69565
LV	P7		0.12	5.99	7.9275	1.323456	66.0625
LV	P8		0.115	6.1275	8.6575	1.412893	75.28261
HV	P1	14.3	0.0375	1.865	3.57	1.914209	95.2
HV	P2	9	0.1375	7.065	7.9975	1.131989	58.16364
HV	P3	11.2	0.07	3.8525	5.4825	1.423102	78.32143
HV	P4	7.9	0.1425	7.155	8.82	1.232704	61.89474
HV	P5		0.085	7.24	7.03	0.970994	82.70588
HV	P6		0.08	3.93	6.0525	1.540076	75.65625
HV	P7		0.0925	3.685	10.6625	2.893487	115.2703
HV	P8		0.1175	6.0875	9.21	1.512936	78.38298

Data Collection for 26.07.2017

		Proximal sensing single leaves: basal, media, alta, lateral											
Vigour	Plant	$\overline{x}$ Tmin basal	$\overline{x}$ Tmax basal	$\overline{x}$ Tmed basal	$\overline{x}$ Tmin media	$\overline{x}$ Tmax media	$\overline{x}$ Tmed media	$\overline{x}$ Tmin alta	$\overline{x}$ Tmax alta	$\overline{x}$ Tmed alta	$\overline{x}$ Tmin lateral	$\overline{x}$ Tmax lateral	$\overline{x}$ Tmed lateral
LV	P1	33.6	37.2	35.7	31.2	36.1	34.1	28.4	31.6	30.1	30	33.7	32.2
LV	P2	30.2	34.2	32.5	31.2	34.8	33.2	29.3	32.2	31.1	28.0	30.7	29.8
LV	P3	33.7	37.9	35.5	32.7	35	34.1	32.1	33.5	33.0	29.9	32.3	31.3
LV	P4	33.4	35.3	34.5	32.7	36.2	34.6	28.9	33.5	31.7	24.6	29.7	29.0
LV	P5	30.6	32.7	31.6	28.6	30.4	29.8	27.9	29.8	28.8	27.1	28.6	28.9
LV	P6	30.6	34.8	32.7	30.7	33.2	31.8	28.5	31.3	30.6	27.9	30.0	29.3
LV	P7	28.8	31.8	30.7	28.9	31.1	30.3	28.4	30.0	29.4	28.4	30.9	29.7
LV	P8	32.9	37.9	36.2	29.7	31.8	30.9	28.2	30.2	29.3	28.5	30.7	29.6
HV	P1	35.9	41.0	39.3	32.5	39.7	35.5	29.9	34.5	32.3	31.3	34.0	32.8
HV	P2	31.5	37.6	34.1	30.6	35	32.1	29.6	32.7	31.5	28.4	30.5	29.5
HV	P3	36.2	42.1	40.2	33.3	37.3	35.5	34.9	40.7	32.9	32.1	33.7	32.1
HV	P4	32.3	37.0	34.5	32.6	37.5	34.7	29.1	32.8	31.0	30.8	33.5	32.3
HV	P5	34.3	40.0	37.0	33	35.0	34.5	32.0	36.9	32.3	29.1	31.2	30.3
HV	P6	32.2	34.5	33.2	29.2	31.6	30.2	30.4	33.3	31.8	31.5	34.0	32.6
HV	P7	35.5	39.9	37.7	32.0	36.0	33.9	32.0	34.6	33.4	33.2	34.6	33.9
HV	P8	33.1	37.3	35.1	31.4	34.5	33.0	29.5	33.6	31.3	27.5	30.0	29.1

		Proximal sensing canopy (zones): South exposed, North exposed							
Vigour	Plant	Tmed S Canopy basal	Tmed S Canopy media	Tmed S Canopy alta	Tmed S Canopy	Tmed N Canopy basal	Tmed N Canopy media	Tmed N Canopy alta	Tmed N Canopy
LV	P1	35.6	32.5	32.4	33.5	33.7	30.7	30.1	31.5
LV	P2	34.9	31.8	31.2	32.6	33.7	30.5	29.7	31.3
LV	P3	33.9	32.1	31.3	32.4	34.1	31.6	31.8	32.5
LV	P4	35.4	31.7	31.7	32.9	31.8	30.2	29.9	30.6
LV	P5	32.6	30.5	29.5	30.9	29.6	28	27.3	28.3
LV	P6	31.6	29.7	28.9	30.1	29.2	28.5	28.1	28.6
LV	P7	30.6	29.6	28.6	29.6	30.1	30.1	29.1	29.8
LV	P8	32.9	30.2	29.7	30.9	30.3	28.9	28.7	29.3
HV	P1	35.4	33.6	33	34	33.7	32.7	32.7	33.0
HV	P2	33.8	31.2	30.5	31.8	31.3	29.4	33	31.2
HV	P3	35.7	32.5	32	33.4	34.2	33.4	32.8	33.5
HV	P4	33.4	30.3	29.8	31.2	31.9	29.8	29	30.2
HV	P5	35	34.8	32.6	34.1	32.8	31.2	30.8	31.6
HV	P6	32.4	31	30.6	31.3	33	32	31.4	32.1
HV	P7	36.1	34.4	33.8	34.8	33.2	31.5	30.9	31.9
HV	P8	32.3	31.4	30.9	31.5	31.1	29.8	29.7	30.2

		Reference leaves						
Vigour	Plant	x̄ Tmin RIFcaldo	x̄ Tmax RIFcaldo	x̄ Tmed RIFcaldo	x̄ Tmin RIFfreddo	x̄ Tmax RIFfreddo	x̄ Tmed RIFfreddo	Ig-Index
LV	P1	32.5	37.4	34.7	19.8	23.5	21.3	0.9
LV	P2	33.8	42.4	38.4	21.0	25.9	23.4	0.6
LV	P3	32.6	37	34.4	22.9	30.1	26	0.8
LV	P4	31.9	38.3	35.2	20.9	27.4	23.0	0.8
LV	P5	29.7	32.5	30.9	20.9	26.3	23.5	1
LV	P6	30.4	33.2	31.7	20.3	27.4	23.0	0.8
LV	P7	29.9	33.9	32.1	22	28.9	24.9	0.6
LV	P8	29.8	37.9	33.5	22.0	27.4	24.7	0.7
HV	P1	33.6	40.3	36.8	21.1	27.4	22.8	0.8
HV	P2	34.7	40.4	37.2	23.1	28.5	25.4	0.5
HV	P3	33.5	40.5	35.6	22.3	27.8	24.4	0.8
HV	P4	34.5	42.0	38.9	21.6	27.4	23.6	0.5
HV	P5	34.2	39.1	36.4	22	27.6	24.3	0.9
HV	P6	32.9	39.5	35.5	23.4	28.3	25.4	0.6
HV	P7	35.3	42.3	38.4	21.1	25.8	23.0	0.8
HV	P8	31.9	38.3	35.4	20.2	27	23.1	0.7

		Remote sensing	Thermal data and comparisons			
Vigour	Plant	Tdrone	Tair	VDP	Td-Ta	Td-Tc
LV	P1	34.7	30.2	2935	4.5	1.2
LV	P2	33.8	30.2	2901	3.6	1.2
LV	P3	33.3	30.2	2922	3.1	0.9
LV	P4	33.1	30.2	2911	2.9	0.2
LV	P5	34.9	30.2	2964	4.7	4.0
LV	P6	33	30.2	2911	2.8	2.9
LV	P7	31.2	30.2	2942	1	1.6
LV	P8	32.8	30.2	2907	2.6	1.9
HV	P1	31.8	30.2	3108	1.6	-2.2
HV	P2	29.4	30.2	3116	-0.8	-2.4
HV	P3	31.7	30.2	3081	1.5	-1.7
HV	P4	29.5	30.2	3090	-0.7	-1.7
HV	P5	30.2	30.2	3159	0	-3.9
HV	P6	30.7	30.2	3149	0.5	-0.6
HV	P7	33.4	30.2	3153	3.2	-1.4
HV	P8	29.4	30.2	3114	-0.8	-2.1

		Plant physiological parameters						
Vigour	Plant	ΨPLWP	ΨLWP	g_s	E	A	WUE A/E	WUE A/gs
LV	P1	5.6	14.2	0.045	2.5775	4.8575	1.884578	107.9444444
LV	P2	5.1	13.7	0.05	3.3275	3.97	1.193088	79.4
LV	P3	5.7	13.9	0.0425	2.745	3.6925	1.345173	86.88235294
LV	P4	5.9	13.4	0.04	2.57	2.8775	1.11965	71.9375
LV	P5			0.035	3.79	4.875	1.28628	139.2857143
LV	P6			0.0425	2.66	3.605	1.355263	84.82352941
LV	P7			0.055	3.4725	4.44	1.278618	80.72727273
LV	P8			0.0425	2.945	3.7175	1.262309	87.47058824
HV	P1	5.4	12.8	0.0225	1.4175	2.375	1.675485	105.5555556
HV	P2	2.8	11.1	0.1075	4.105	9.7275	2.369671	90.48837209
HV	P3	5.9	12.3	0.0375	2.605	3.59	1.378119	95.73333333
HV	P4	1.9	7.9	0.1225	5.2725	9.49	1.799905	77.46938776
HV	P5			0.0475	2.555	3.6525	1.42955	76.89473684
HV	P6			0.0725	4.415	6.1475	1.392412	84.79310345
HV	P7			0.045	2.9675	3.8125	1.284751	84.72222222
HV	P8			0.119	3.8525	5.5425	1.438676	46.57563025